Photochemical Fate of Solvent Constituents of Corexit Oil Dispersants

by

Stephanie C. Kover

B.S., University of Nevada Reno, 2011

A thesis submitted to the

Faculty of the Graduate School of the University of Colorado

in partial fulfillment of the requirement for the degree of

Master of Science

Department of Civil, Environmental, and Architectural Engineering

2013

This thesis entitled:

Photochemical Fate of Solvent Constituents of Corexit Oil Dispersants

written by Stephanie C. Kover has been approved for the

Department of Civil, Environmental, and Architectural Engineering

_____

Karl Linden

_____

Fernando Rosario-Ortiz

_____

Kaelin Cawley

Date_____

The final copy of this thesis has been examined by the signatories, and we

Find that both the content and the form meet acceptable presentation standards

Of scholarly work in the above mentioned discipline.

Kover, Stephanie Claire (M.S., Civil Environmental, and Architectural Engineering)

Photochemical Fate of Solvent Constituents of Corexit Oil Dispersants

Thesis directed by Fernando Rosario-Ortiz and Karl Linden

In 2010, an estimated 1.87 million gallons of chemical dispersants were applied to open ocean waters in Gulf of Mexico as part of the response to the Deepwater Horizon blowout. This unprecedented volume of dispersant application highlighted the importance of dispersant chemical formulations, raising questions of dispersant fate and transport in the open ocean and spurring research into formulation improvements. The research presented here elucidates the contribution of sunlight-driven processes to the degradation of solvent constituents of these dispersant mixtures to aid in optimizing the operational effectiveness. Specifically, the compounds propylene glycol (PG) and 2-butoxyethanol (2-BE) were examined. A series of photodegradation experiments were conducted to determine the contribution of direct photolysis and indirect photolysis via hydroxyl radical ($HO^{\bullet}$) to compound degradation. Experiments were performed using both a low pressure (LP) and medium pressure (MP) mercury vapor ultraviolet (UV) lamp system, and a solar simulator. Sample matrices included ultrapure water, nitrate amended water, hydrogen peroxide (H_2O_2) spiked water, Gulf of Mexico seawater, and Boulder Creek surface water. Preliminary experiments included determination of the molar absorption coefficients (ε) and the $HO^{\bullet}$ reaction rate constants ($k_{HO\bullet}$) of the individual compounds. This research found that significant direct photolysis of either PG or 2-BE from sunlight is unlikely. The $k_{HO\bullet}$ for PG and 2-BE were determined to be 6.15×10^8 M^{-1} s^{-1} and 1.15×10^9 M^{-1} s^{-1},

respectively. Solar simulation and UV experiments indicate that in natural systems, neither PG nor 2-BE is expected to undergo significant, rapid degradation due to direct or indirect photolysis. PG and 2-BE are effectively degraded through indirect photolysis in the presence of high $HO^{\bullet}$ concentrations, as witnessed in the UV/H_2O_2 experiments conducted in this study, suggesting UV/H_2O_2 is a feasible alternative for the treatment of waters containing PG and 2-BE.

Acknowledgements

I would like to acknowledge my advisors, Fernando Rosario-Ortiz and Karl Linden, for all of their advice and office hours spent on this project. I would also like to thank my labmates for their support. I would like to especially acknowledge doctoral student Caitlin Glover, doctoral student Simón Mostafa, and post-doctoral student Eunkyung Lee for sharing their analytical and laboratory knowledge with me. Caitlin Glover also contributed to this thesis with the quantification of the formation rate of hydroxyl radical in Gulf of Mexico seawater. Mei Mei Dong contributed the formation rate of hydroxyl radical in Boulder Creek water.

This research was made possible by a grant from BP/The Gulf of Mexico Research Initiative. Grant # SA 12-05/GoMRI-002.

Table of Contents

1. Introduction……..1

2. Materials and Methods……...10

2.1 Experimental design……....10

2.2 Chemicals and reagents……...……11

2.3 UV and solar simulation systems……...…….13

2.4 Experimental Methods……15

2.4.1 Molar absorption coefficients…….……15

2.4.2 Hydroxyl radical reaction rate constants……16

2.4.3 UV experiments……..18

2.4.4 Solar simulation experiments…….……19

2.5 Analytical methods…….20

2.5.1 GC-FID analysis……...20

2.5.2 HPLC-UV analysis……...22

3. Results……24

3.1 Molar absorption coefficients…….…24

3.2 Hydroxyl radical reaction rate constants…….25

3.3 UV experiments……...….27

3.4 Solar simulation experiments……..32

4. Discussion……..34

4.1 Molar absorption coefficients and direct photolysis potential……34

4.2 Comparison of experimental and estimated $k_{HO^{\bullet}}$ values…….35

4.3 Implications of Solar Simulation, UV, and UV/AOP experiment results……...37

References……..45

Appendix A……49

Appendix B……52

Appendix C……56

List of Tables

Table 1: Chemical constituents of Corexit 9500 and 9527……..……....2

Table 2: Reported aerobic propylene glycol half-lives…….....5

Table 3: Reported anaerobic propylene glycol half-lives……6

Table 4: Characterization of sample waters used as experimental matrices……..12

Table 5: Analytical techniques used to quantify concentrations of experimental compounds…..22

Table 6: Hydroxyl radical reaction rate constants for propylene glycol and 2-butoxyethanol……..…....25

Table 7: Statistical significance of observed differences in propylene glycol degradation with LP UV/H_2O_2 in varying matrices……...……...……..…37

Table 8: Statistical significance of observed differences in 2-butoxyethanol degradation with LP UV/H_2O_2 in varying matrices……...……...……38

Table A-1: Reported $HO^{\bullet}$ steady state concentrations, formation rates, and source contributions in seawaters of varying type…….……..50

Table A-2: Reported $HO^{\bullet}$ steady state concentrations, formation rates, and source contributions in surface waters of varying type…….…….....…51

Table C-1: Relative standard deviation (RSD) determination……..57

List of Figures

Figure 1: Irradiance spectrum of solar simulator compared to natural sunlight……...……14

Figure 2: GC-FID chromatograms of propylene glycol and 2-butoxyethanol…….....21

Figure 3: HPLC-UV chromatogram of para-chlorobenzoic acid (pCBA)……...23

Figure 4: Molar absorption coefficients (ε) for propylene glycol and 2-butoxyethanol as a function of wavelength……..24

Figure 5: Results of competition kinetics experiments as a function of UV dose……....26

Figure 6: Propylene glycol in natural waters does not significantly degrade with the application of low or medium pressure UV…….…….28

Figure 7: 2-Butoxyethanol in natural waters does not significantly degrade with the application of low or medium pressure UV…….….29

Figure 8: UV/H_2O_2 advanced oxidation processes in ultrapure water degrade propylene glycol and 2-butoxyethanol…….....30

Figure 9: Observed degradation rates of propylene glycol and 2-butoxyethanol in natural waters treated with UV/H_2O_2…….……...31

Figure 10: No observed indirect photolysis of propylene glycol or 2-butoxyethanol with solar simulation in nitrate amended solution……..…....33

Figure 11: Comparison of hydroxyl radical reaction rate constants ($k_{HO\bullet}$) obtained experimentally and estimated using a group contribution method……...…..36

Figure 12: Comparison of modeled decay and experimental data points for PG in three different matrices…….……...…..39

Figure 13: Comparison of modeled decay and experimental data points for 2-BE in three different matrices…….…….……...…..40

Figure 14: Percent removal as a function of $[HO^{\bullet}]_{ss}$ and exposure time (Ct)…….…….…..42

Figure B-1: Formation of phenol from irradiated crude oil indicates formation of hydroxyl radical……...…….…….54

Figure B-2: Singlet oxygen production as a function of film thickness……55

Figure C-1: Importance of inherent standard deviation in reporting results of a propylene glycol competition kinetics experiment…….……..….58

List of Equations

Equation 1: Determining molar absorption coefficients (ε) as a function of wavelength…….15

Equation 2: Determining hydroxyl radical reaction rate constant using competition kinetics…..16

Equation 3: Determining experimental hydroxyl radical steady state concentrations……...18

Equation 4: Determining percent removal of a compound as a function of $[HO^{\bullet}]_{ss}$ and time…...41

1. Introduction

In 2010, an estimated 1.87 million gallons of the chemical dispersants Corexit 9500 and 9527 were applied to open ocean waters in Gulf of Mexico as part of the response to the Deepwater Horizon blowout (Kujawinski *et al.* 2011, Hayworth and Clement 2012). This unprecedented volume of dispersant application highlighted the importance of dispersant chemical formulations, raising questions of dispersant fate and transport in the open ocean and spurring research into formulation improvements. Prior to the Deepwater Horizon blowout, the chemical compositions of most chemical dispersants were proprietary information. In 2010, the compositions of the Corexit dispersants were released to the EPA; the constituents and their functions within the formulations are listed in Table 1. Chemical dispersants are comprised of two main constituent groups: surfactants and solvents. In Corexit 9500 and 9527, dioctyl sodium sulfosuccinate (DOSS) is an anionic surfactant. Span 80, Tween 80, and Tween 85 are nonionic surfactants. Propylene glycol (PG) and 2-butoxyethanol (2-BE) are main solvent components of the mixtures, along with dipropylene glycol monobutyl ether (DPnB) and other petroleum distillates (EPA 2010). Solvents are key constituents of any dispersant formulation. Solvents aid in delivery of the active ingredients (surfactants such as DOSS) in dispersant mixtures, and also allow these surfactants to penetrate the oil films and get to the water-oil interface where micelles can be formed, increasing bioavailability and biodegradation of the oil.

Table 1: Chemical constituents of Corexit 9500 and 9527.

CAS Registry Number	Chemical Name	Short Name	Function
57-55-6	Propylene glycol	PG	Solvent
111-76-2*	2-Butoxyethanol	2-BE	Solvent
577-11-7	Dioctyl sodium sulfosuccinate	DOSS	Surfactant
1338-43-8	Sorbitan, mono-(9Z)-9-octadecenoate	Span 80	Surfactant
9005-65-6	Sorbitan, mono-(9Z)-9-octadecenoate, poly(oxy-1,2-ethanediyl) deriviatives	Tween 80	Surfactant
9005-70-3	Sorbitan, tri-(9Z)-9-octadecenoate, poly(oxy-1,2-ethanediyl) deriviatives	Tween 85	Surfactant
29911-28-2	Dipropylene Glycol Monobutyl Ether	DPnB	Solvent
64742-47-8	Petroleum distillates		Solvent

* *Not a component of Corexit 9500*

One aspect contributing to the overall effectiveness of a dispersant mixture is the operational effectiveness. Operational effectiveness monitors how efficiently the dispersant is applied and penetrates the oil film. Of the 1.87 million gallons of Corexit applied in response to the Deepwater Horizon Blowout, 1.1 million gallons (59%) were applied at the surface and in direct contact with sunlight during the application process (Hayworth and Clement 2012). If any of the Corexit constituents were degraded due to this solar exposure, the operational efficiency of Corexit would be reduced. Despite this potential impact, the photochemical fates of the chemical constituents of Corexit 9500 and 9527 remain relatively unexplored. Previous research by this lab group (not described here) has intensively investigated the photodegradation of the surfactant DOSS and DPnB.

The research presented here elucidates the contribution of sunlight-driven processes to the degradation of solvent constituents of these dispersant mixtures to aid in optimizing the operational effectiveness with respect to application. Specifically, the compounds PG and 2-BE were examined. If solvents such as PG and 2-BE were rapidly photodegraded upon surface

application, dispersant mixtures that are applied may not work as designed, resulting in reduced response efficiency, increased lag time for biodegradation of oil, and increased cost. Small changes made to solvent concentration based on spill location and solar flux may prevent such unnecessary over-application.

Propylene glycol and 2-BE are also used for many other industrial applications other than oil dispersal, and thus have potential to be present in many natural waters. Therefore, an understanding of the photochemical fates of these two compounds can be applied to treatment and/or application scenarios other than optimization of oil dispersant application. A brief review of information regarding major uses, toxicity, and reported degradation rates is presented below for each compound.

Propylene Glycol

Propylene glycol is a compound commonly used as a functional fluid for its solvency properties and its widespread use provides ample opportunity for unintentional release to natural waters. It is important to understand that one reason for the abundance of PG use is the low toxicity exhibited by the compound. Under US FDA classification, PG is registered as GRAS (Generally Recognized as Safe) (ATSDR 1997). The EPA benchmark for aquatic life for PG is relatively high at 500 mg L^{-1} (Team 2010). Although PG poses no immediate toxicological threats to aquatic life, it has a high chemical oxygen demand (COD), requiring 1.68 g COD per g propylene glycol. Due to the abundance in application use, oxygen depletion may occur in waters and soils exposed to high concentrations of PG (Veltman *et al*. 1998).

The largest industrial use of concern is the use of PG in aircraft deicing fluids. About 4,000 L of deicing fluid are required to service a typical large jet (Castro *et al.* 2001) and it is estimated that deicing fluid usage is 11 million gallons per season, only accounting for the 20 largest airports (Corsi *et al.* 2001). Aircraft deicing fluids are applied at temperatures below freezing and frequently during storm events. Propylene glycol is a very hydrophilic compound due to the presence of two alcohol functional groups. This compound has a very low octanol-water partition coefficient ($K_{ow} = 10^{-0.92}$) and is miscible in water (ATSDR 1997). These properties, coupled with the significant storm runoff typical during an aircraft deicing fluid application, create a disconcerting scenario for transport of PG into receiving water bodies. For these reasons, aircraft deicing fluid waste containing high concentrations of PG often requires treatment prior to discharge to natural waters.

Reported aerobic degradation half-lives for PG are listed in Table 2 and range from as short as 0.35 days (soil pan amended with activated sludge at 22°C and pH 7) to as long as 292

days (topsoil at -2°C and pH 7.2). If storm runoff contains a high concentration of aircraft deicing fluid, it is likely that the large oxygen demand of PG will quickly deplete available electron acceptors, the final result of which is an anaerobic environment (Schoenberg *et al.* 2001). Hence, anaerobic biodegradation of PG is the degradation mechanism most frequently found in literature, with reported half-lives from studies of suspended growth fill-draw reactors, soil pans, and soil columns (Table 3). Reported half-lives range from 0.20 days to 10.9 days at the lowest tested temperature of 4°C. Both aerobic (Klecka *et al.* 1993) and anaerobic (Schoenberg *et al.* 2001, Jaesche *et al.* 2006) processes have been shown to be inhibited at low temperatures, either resulting in slowed degradation kinetics or incomplete mineralization. Due to the inhibition of biological degradation at the low temperatures encountered during aircraft deicing fluid use, non-biological photochemical processes could play a larger role in overall PG degradation. An understanding of the photochemical fate of PG would aid in optimizing secondary collection and treatment of aircraft deicing fluids.

Table 2: Reported aerobic propylene glycol half-lives.

Half-Life	Temp/pH	Inoculum Media	Initial Conc.	Spike Form	Reference
0.35 d[a]	22°C/7	Soil Pan + Sludge	4210 ppm	ADF	(Bausmith and Neufeld 1999)
3.9 d[a]	25°C/7.2	Topsoil	650 ppm	Glycol mix	(Klecka *et al.* 1993)
4.3 d[a]	22°C/4.5	Soil Pan + Sludge	4210 ppm	ADF	(Bausmith and Neufeld 1999)
4.3 d[a]	22°C/7	Soil Pan	4210 ppm	ADF	(Bausmith and Neufeld 1999)
5.6 d[b]	20.9°C/7.44	Activated Sludge	5000 ppm	PG	(West *et al.* 2007)
11.6 d[a]	22°C/4.5	Soil Pan	4210 ppm	ADF	(Bausmith and Neufeld 1999)
13.6 d[b]	20.8°C/8.11	Seawater	5000 ppm	PG	(West *et al.* 2007)
22.1 d[a]	8°C/7.2	Topsoil	1004 ppm	ADF avg.	(Klecka *et al.* 1993)
292 d[a]	-2°C/7.2	Topsoil	1342 ppm	ADF avg.	(Klecka *et al.* 1993)

[a] *determined from direct measurement of propylene glycol*
[b] *determined from CO_2 formation*

Table 3: Reported anaerobic propylene glycol half-lives.

Half-Life	Temp/pH	Inoculum Media	Initial Conc.	Spike Form	Reference
0.20 d[b]	35°C/neutral	Fill/Draw Reactor	5351 ppm PG	ADF	(Schoenberg *et al.* 2001)
0.36 d[b]	25°C/neutral	Fill/Draw Reactor	5351 ppm PG	ADF	(Schoenberg *et al.* 2001)
1.25 d[a]	20°C/7.5-8	Gravel-rich Topsoil	500 ppm PG	PG	(Jaesche *et al.* 2006)
3.2 d[a]	22°C/7	Soil Pan + Sludge	4210 ppm PG	ADF	(Bausmith and Neufeld 1999)
5.3 d[a]	22°C/4.5	Soil Pan + Sludge	4210 ppm PG	ADF	(Bausmith and Neufeld 1999)
6.3 d[a]	22°C/7	Soil Pan	4210 ppm PG	ADF	(Bausmith and Neufeld 1999)
7.8 d[a]	4°C/7.5-8	Gravel-rich Topsoil	500 ppm PG	PG	(Jaesche *et al.* 2006)
9.9 d[a]	22°C/4.5	Soil Pan	4210 ppm PG	ADF	(Bausmith and Neufeld 1999)
10.9 d[a]	4°C/7.5-8	Gravel-rich Topsoil	50 ppm PG	PG	(Jaesche *et al.* 2006)

[a] *determined from direct measurement of propylene glycol*
[b] *determined from COD*

2-Butoxyethanol

2-Butoxyethanol is commonly used in the manufacture of industrial and commercial household products. Some examples of the manufacturing uses of 2-BE include lacquers, cleaning products, paints, paint thinners, textiles, and dry-cleaning compounds (ATSDR 1998). This prevalence of use provides ample opportunity for 2-butoxyethanol to be introduced to natural waters. Potential pathways for 2-BE release into the environment include waste streams from manufacturing facilities, return water from industrial operations, and leachate from landfills and hazardous waste sites (ATSDR 1998). This compound is also hydrophilic, with a low octanol-water partition coefficient ($K_{ow} = 10^{0.83}$) (ATSDR 1998), making it highly mobile in soil and further facilitating transport of the compound to receiving waters. 2-Butoxyethanol has also been shown to be slightly toxic to blue-green algae and oysters (*Crassotera virginicas*) with acute exposure (European Centre for Ecotoxicology and Toxicology of 1994). The EPA has set the benchmark for aquatic life for 2-BE at 0.165 mg L^{-1} (Team 2010). These associated toxicity concerns make maintaining 2BE-free waters of ecological importance.

Due to its widespread and varied uses coupled with its chemical properties, 2-BE is likely to be present in waters undergoing engineered treatment. 2-Butoxyethanol has been detected in drinking water seven major cities, stormwater, wastewater, and finished water from advanced waste treatment plants (Hayworth and Clement 2012, ATSDR 1998, McPherson *et al.* 2005). Contamination can be at extreme levels, as was the case involving the Hayashida River which was contaminated from leather manufacturing; detected concentrations of 2-BE were as high as 5.68 mg L^{-1} (Yasuhara *et al.* 1981). The demonstrated presence of 2-BE in both untreated and treated waters illustrates that it is likely to present in waters that will undergo treatment, but also suggests that current treatment techniques are not be effective at removal.

Yet, surprisingly few studies have addressed the degradation of 2-BE. One environmental study has shown that 2-BE is readily aerobically biodegradable with a reported half-life in surface water of 7-28 days (ATSDR 1998). No published research investigates the effects of photochemical processes. A deeper understanding of the photochemical fate of 2-BE would remedy this gap in knowledge and could also be broadened to include photochemical treatment scenarios, potentially increasing 2-BE removal in engineered systems.

Summary

No published study investigates the photodegradation of either PG or 2-BE in natural waters or engineered treatment systems. As these solvent compounds have key functions within oil dispersant formulations, photochemical processes could impact the operational effectiveness of dispersants such as Corexit during surface applications such as was done in response to the Deepwater Horizon Blowout. To understand possible solar effects, this study investigated the contributions of sunlight-driven direct and indirect photolysis to PG and 2-BE degradation in seawater.

The industrial use of PG and 2-BE is not limited to dispersant formulations. Propylene glycol and 2-BE may be transported to water bodies other than seawater from manufacturing waste streams, landfill leachate, or uncontained aircraft deicing fluids. As these compounds may be targeted for treatment in an engineered system, this study also performed analysis of PG and 2-BE degradation using ultraviolet (UV) treatments and UV/ advanced oxidation processes (AOP) in multiple water matrices for a more comprehensive understanding of photochemical fate.

2. Materials and Methods

2.1 Experimental design

A series of photodegradation experiments were conducted to determine the contribution of direct photolysis and indirect photolysis via hydroxyl radical to compound degradation. Experiments were performed using both a low pressure (LP) and medium pressure (MP) mercury vapor UV lamp system, and a solar simulator. Sample matrices included ultrapure water, nitrate amended water, hydrogen peroxide (H_2O_2) spiked water, Gulf of Mexico seawater, and Boulder Creek surface water. Preliminary experiments to develop information on the fundamental photochemical parameters included determination of the molar absorption coefficients (ε) and the hydroxyl radical ($HO^{\bullet}$) reaction rate constants ($k_{HO\bullet}$) of the individual compounds.

2.2 Chemicals and reagents

Hydrogen peroxide, bovine catalase, and propylene glycol (Sigma-Aldrich, St. Louis, MO); para-chlorobenzoic acid (ICN Biomedicals Inc., Aurora, OH); sodium nitrate and sodium phosphate (Fisher Scientific, Fair Lawn, NJ); and 2-butoxyethanol (Alfa Aesar, Ward Hill, MA) were all of reagent grade purity. Hydrogen peroxide, 2-butoxyethanol, and propylene glycol stock solutions were created and stored in amber glass bottles at 4°C. Ultrapure water (arium611-VF, Sartorium Stedium, Bohemia, NY) was used for stock solutions. Due to aqueous instability, true H_2O_2 stock solution concentrations were determined prior to each experiment using a triiodide method (Klassen *et al.* 1994). Gulf of Mexico seawater was collected 12-02-2011 offshore of Terrebonne Bay, LA in the Gulf of Mexico and stored in amber glass bottles at 4°C. Boulder Creek water, used to represent a typical surface water, was collected 02-06-2013 from Ebben G. Fine Park, Boulder, CO and stored in amber glass bottles at 4°C. Seawater and surface water used in this study were characterized for pH, alkalinity, nitrate concentration ($[NO_3^-]$), nitrite concentration $[NO_2^-]$), dissolved organic carbon (DOC) and $HO^{\bullet}$ formation rate ($R_{HO\bullet}$) (Table 4). Alkalinity was determined using a Hach titrator; nitrate and nitrite concentrations were determined using Hach kits TNT839 and TNT835, respectively (Hach, Loveland, CO). DOC was measured with a Shimadzu TOC-V_{CSH} organic carbon analyzer (Shimadzu America, Inc. Columbia MD). $R_{HO\bullet}$ was determined using the benzene to phenol probe method developed by Mopper and Zhou (1990) and described in detail by Dong and Rosario-Ortiz (2012).

Table 4: Characterization of sample waters used as experimental matrices.

Parameter	Units	Seawater Gulf of Mexico	Surface Water Boulder Creek
$R_{HO\bullet}$	$\times 10^{-12}$ M s^{-1}	2.3	15.0
pH		7.8	7.35
Alkalinity	mg L^{-1} $CaCO_3$	92	32.8
$[NO_3^-]$	mg L^{-1} NO_3^- - N	BD	0.083
$[NO_2^-]$	mg L^{-1} NO_2^- - N	0.011	0.013
DOC	mg_C L^{-1}	1.620	1.751

$R_{HO\bullet}$: hydroxyl radical formation rate; BD: below detection; DOC: dissolved organic carbon

2.3 UV and solar simulation systems

The LP UV bench system contained 4 ozone-free 15 W mercury lamps (#G15T8). The MP UV bench system (Calgon Carbon Corp., Pittsburg, PA) contained a 1 kW mercury lamp. Both systems were quasicollimated using a cylindrical tube (6.4 cm diameter, 10 cm length). The emission spectra of the two lamps are shown in Figure 4. Crystallization dishes were used as exposure vessels in which the sample was continuously stirred. UV exposure times to achieve a specific UV dose were determined using the method developed by Bolton and Linden (2003) which corrects measured incident irradiance by factors including absorbance, depth, and dish diameter to calculate the average irradiance in a completely mixed batch system. Sample surface irradiance was measured using an IL-1700 radiometer (Peabody, MA). Sample absorbance was measured using a Varian Cary100Bio spectrophotometer (Agilent, Santa Clara, CA).

Solar simulation experiments were conducted using a Model 94041 Oriel solar simulator equipped with a 1000 W lamp and air mass 1.5 global filter (Newport Corp., Oriel Instruments, Stratford, CT). The total irradiance was 68 W m^{-2} for the wavelength range of 290 to 400 nm. This is close to the total irradiance for natural sunlight on a clear summer day in Boulder, CO at noon (55 W m^{-2}), and about double that at 9 am (27 W m^{-2}). The irradiance spectrum of the lamp

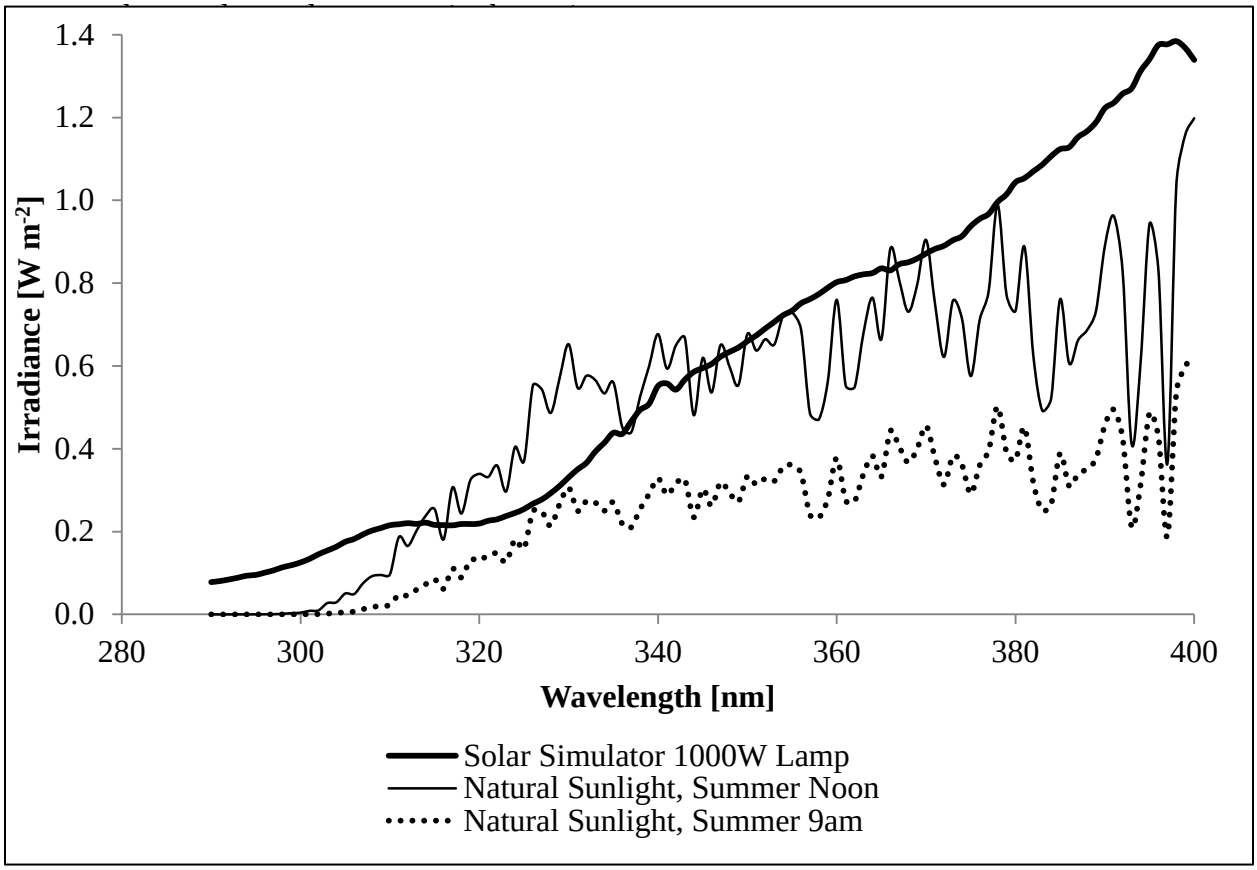

Figure 1. Solar simulator irradiance was measured with a spectrometer USB2000 (Ocean Optics Inc., Florida). Outdoor solar spectrums were obtained through the National Renewable Energy Laboratory's (NREL) Simple Model of the Atmospheric Radiative Transfer of Sunshine (SMARTS) program. Samples exposed to solar simulation were contained in 2 mL pyrex vials with no headspace and exposed while in a water bath maintained at 20°C, below the lamp.

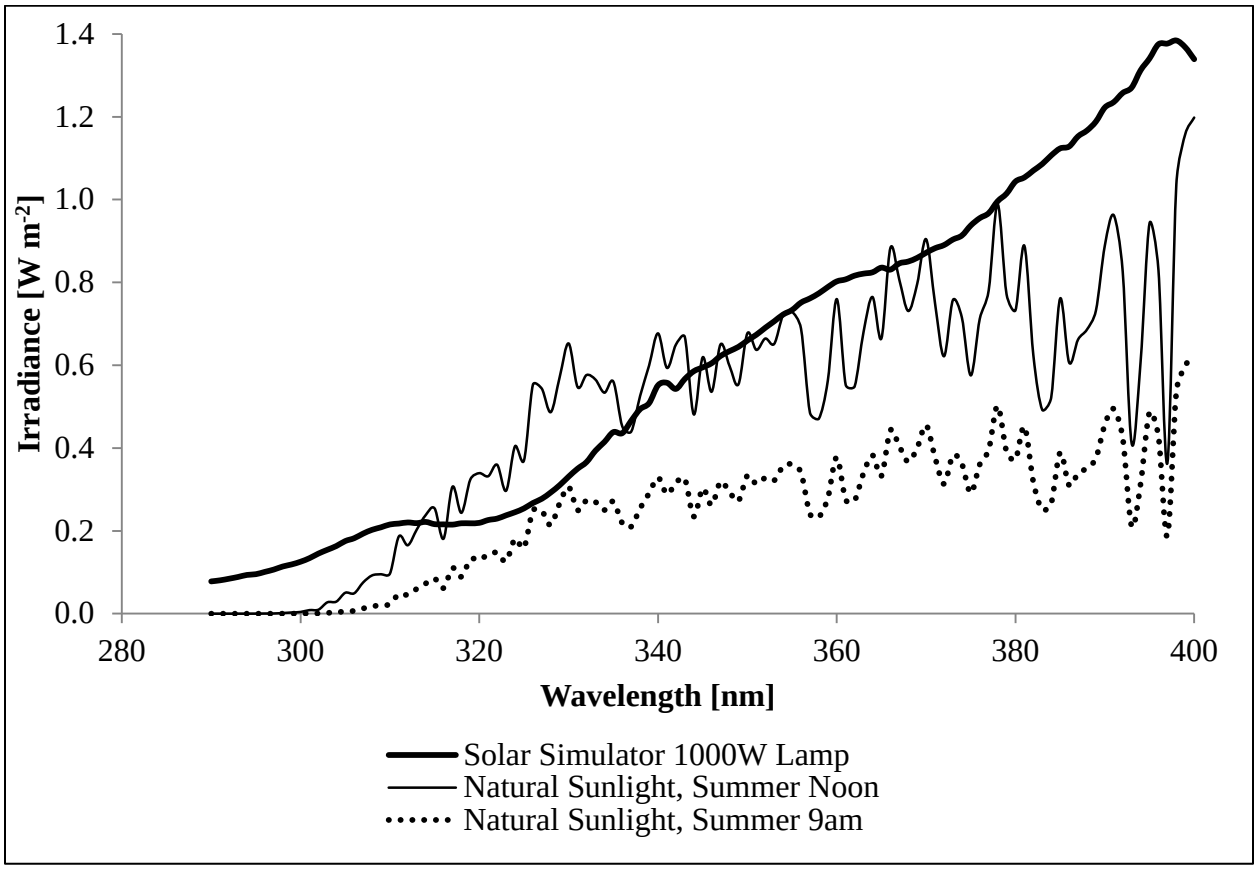

Figure 1: Irradiance spectrum of solar simulator compared to natural sunlight. The solar simulator output (thick solid line) is approximately equivalent to natural summer sunlight at noon (thin solid line) and roughly twice that of natural summer sunlight at 9 am (dashed line).

2.4 Experimental Methods

2.4.1 Molar absorption coefficients

The absorption spectrums for each compound were measured at three different concentrations using a Varian Cary100Bio spectrophotometer (Agilent, Santa Clara, CA). The concentrations were 5 mg L^{-1}, 50 mg L^{-1}, and 500 mg L^{-1} for both PG and 2-BE. A 1 cm path length cuvette was used. Molar absorption coefficients (ε) were determined as a function of wavelength based on the observed change in absorbance with change in concentration (Equation 1). The results are presented in the Results section in Figure 4.

Equation 1: Determining molar absorption coefficients (ε) as a function of wavelength. *A* is sample absorbance, *C* is compound concentration, and *L* is path length. *Adapted from Schwartzenbach et al. (1993).*

$$\varepsilon(\lambda) = \frac{\Delta A(\lambda)}{\Delta C(\lambda) L}$$

2.4.2 Hydroxyl radical reaction rate constants

$k_{HO\bullet}$ were determined using the competition kinetics method described by Shemer *et al.* (2006). Separate experiments were conducted for PG and 2-BE. For the PG experiment, the target compound was spiked at a concentration of 25 mg L^{-1} into 5 mM phosphate buffered ultrapure water. Para-chlorobenzoic acid (pCBA) was used as the probe compound and spiked into the sample matrix at a concentration of 25 mg L^{-1}. For the 2-BE experiment, the target compound and pCBA were spiked at concentrations of 50 mg L^{-1}. Samples were irradiated under LP UV. Probe and target compound degradation due to direct photolysis were monitored after the application of a 1000 mJ cm^{-2} UV dose. Hydrogen peroxide was added to the sample solution at a concentration of 50 mg L^{-1} to create advanced oxidation experimental conditions upon exposure to UV light. Sample aliquots were sacrificed at UV doses of 250, 500, 750, and 1000 mJ cm^{-2}. All sample aliquots were taken in duplicate, quenched with bovine catalase to neutralize residual H_2O_2, transferred to 2 mL vials, and analyzed immediately for pCBA and target compound concentration (either PG or 2-BE). $k_{HO\bullet}$ was determined for each target compound using Equation 2.

Equation 2: Determining hydroxyl radical reaction rate constant using competition kinetics. *Adapted from Shemer et al. (2006).*

$$k_{HO\bullet(target)} = \frac{(k'_{obs(target)} - R_{trans} k'_{d(target)})}{(k'_{obs(pCBA)} - R_{trans} k'_{d(pCBA)})} k_{HO\bullet(pCBA)}$$

The ratio of the observed first order degradation rates of the target compound and pCBA (k'_{obs}) are multiplied by the hydroxyl radical reaction rate of pCBA ($k_{HO\bullet\,(pCBA)}$) which is known to be 5.0×10^9 $M^{-1}s^{-1}$ (Elovitz and von Gunten 1999). The observed first order degradation rates are adjusted for any direct photolysis contributions. The first order direct photolysis rate (k'_d) is multiplied by a transmittance ratio (R_{trans}) to correct for reduced light availability in AOP experiments due to H_2O_2 addition (Shemer *et al.* 2006). These values were compared to estimates obtained using the Group Contribution Method developed by Minakata *et al.* (2009), as well as other reaction rate constants published in the literature (Buxton *et al.* 1988).

2.4.3 UV experiments

UV and UV/AOP experiments were conducted using both LP and MP bench systems. Three sets of photodegradation experiments were conducted using three different matrices: ultrapure water, Gulf of Mexico seawater, and Boulder Creek surface water. For each experimental set, the target compound (either PG or 2-BE) was spiked into the pure matrix at a concentration of 50 mg L^{-1} and irradiated under each UV system. Sample aliquots were sacrificed at predetermined times corresponding to UV doses of 0 and 2000 mJ cm^{-2}. Advanced oxidation processes were then tested by spiking the sample matrix with H_2O_2 (50 mg L^{-1}) as a $HO^{\bullet}$ source. Sample aliquots were sacrificed at predetermined times corresponding to UV doses of 0, 500, 1000, 1500, and 2000 mJ cm^{-2}. All sample aliquots were taken in duplicate, quenched with bovine catalase, and transferred to 2 mL vials. Samples were stored in the dark at 4°C prior to analysis, which occurred within 2 days. Hydroxyl radical steady state concentrations ($[HO^{\bullet}]_{ss}$) were quantified for all experiments using Equation 3 in which the sinks present were the target compounds and $R_{HO\bullet}$ is the quantified value for the given water (Table 4).

Equation 3: Determining experimental hydroxyl radical steady state concentrations. $R_{HO\bullet}$ is the formation rate of hydroxyl radical for the given water. S_i is the concentration of a sink and $k_{HO\bullet(Si)}$ is the hydroxyl radical reaction rate of the sink. *Adapted from Vione et al. (2010).*

$$[HO^{\bullet}]_{ss} = \frac{R_{HO\bullet}}{\sum_i k_{HO\bullet(Si)} S_i}$$

2.4.4 Solar simulation experiments

An indirect photolysis experiment was conducted under solar simulation in NO_3^- amended ultrapure water ($[NO_3^-]$ = 0.01 M). Target compounds were spiked into the matrix at concentrations of 0.0005 M PG and 0.0005 M 2-BE. Prior to irradiation, the sample solution was transferred to individual 2 mL pyrex vials. Samples were irradiated under the solar simulator and sacrificed in duplicate at 29.6 hours, 44.6 hours, 62.6 hours, and 81.6 hours. Due to the length of the experiment and to prevent the simulator from overheating, solar simulation was periodically suspended; samples were stored in the dark at 4°C during these times of non-irradiation. Another solar simulation experiment was conducted using Gulf of Mexico seawater and initial PG and 2-BE concentrations 3.33 mg L^{-1}. Samples were sacrificed in duplicate at 1.25 hours, 3.75 hours, and 7.25 hours. All samples were stored in the dark at 4°C prior to analysis which occurred within a maximum of 3 days. $[HO^{\bullet}]_{ss}$ were quantified for all experiments using Equation 3 in which the sinks present were the target compounds.

2.5 Analytical methods

2.5.1 GC-FID analysis

A method was created to analytically determine PG and 2-BE concentrations using an Agilent 7890A gas chromatograph coupled with a flame ionization detector (GC-FID). An Agilent DB-WAX capillary column (30m x 0.250 mm i.d., 0.25 μm film thickness) was selected to allow direct injection of aqueous samples, minimizing losses associated with the extraction and derivitization processes that would otherwise be required. The method parameters follow: 0.2 uL sample volume was injected into an inlet in splitless mode maintained at 260°C and 17.735 psi. Helium carrier gas was supplied through the column at a flow rate of 1.67 mL/min. The initial oven temperature was 50°C and increased to 220°C at 10°C per min. The FID heater was maintained at 260°C. Hydrogen, air and nitrogen (makeup) gas flows to the detector were 30 mL min^{-1}, 400 mL min^{-1}, and 25 mL min^{-1}, respectively. Under these method conditions, the retention times for 2-BE and PG were 7.46 min and 9.67 min, respectively. Example chromatograms for 50 mg L^{-1} standards are shown in Figure 2. The minimum detection limit for PG and 2-BE under this method were 5 mg L^{-1}, and 2.5 mg L^{-1}, respectively (Table 5). Experiments were engineered to attempt to remain above the practical quantitation limits (PQL) for each compound, set at 5 times the MDL. The PQL for PG is 25 mg L^{-1}; the PGL for 2-BE is 12.5 mg L^{-1}. Relative standard deviations (RSD) ranged from 4% at the PQL (n = 7) to 16% at 50 mg L^{-1} (n = 18) for PG and from 3% near the MDL (n = 7, [2-BE] = 5 mg L^{-1}) to 10% at 50 mg L^{-1} (n = 23) for 2-BE.

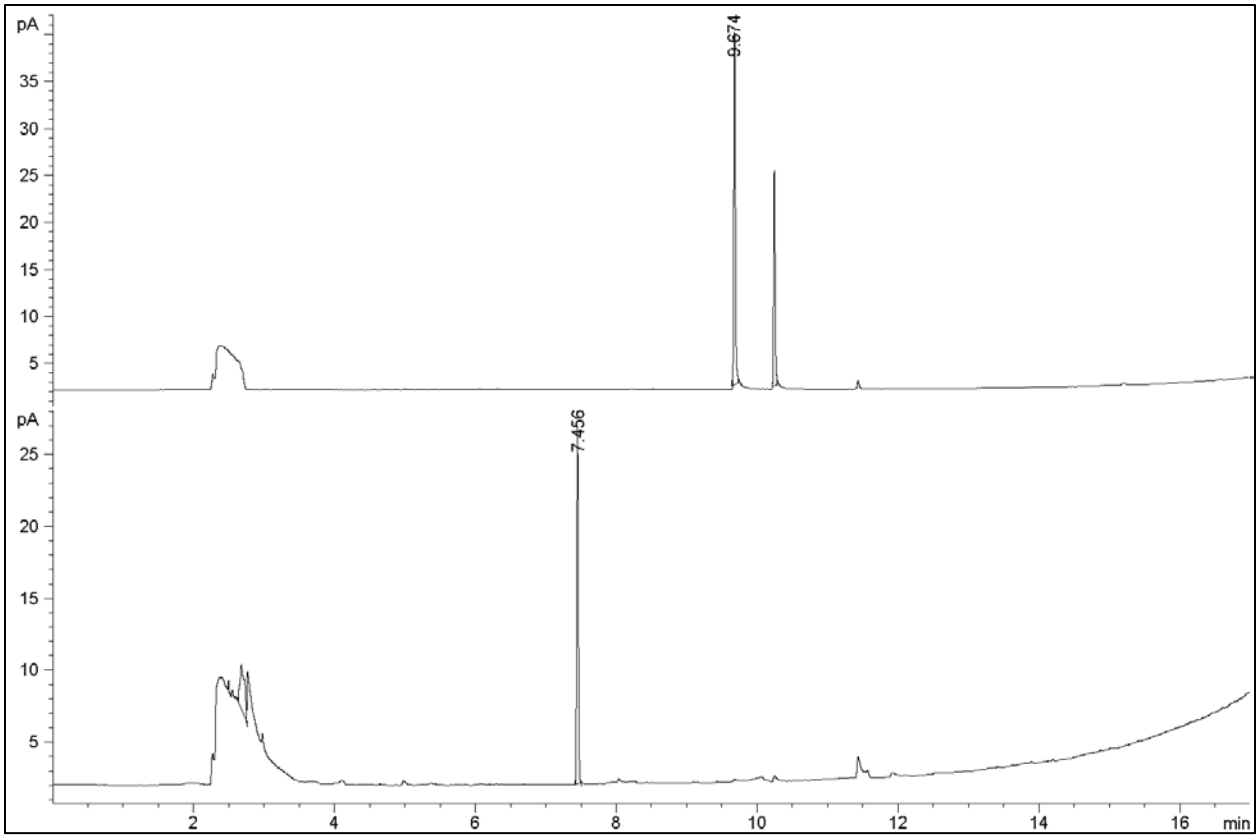

Figure 2: GC-FID chromatograms of propylene glycol (top) and 2-butoxyethanol (bottom). Examples shown are 50 mg L^{-1} concentrations. PG retention time is 9.67 min and 2-BE retention time is 7.46 min using the created direct aqueous injection method.

2.5.2 HPLC-UV analysis

Para-chlorobenzoic acid concentrations were determined using a high performance liquid chromatography-UV (HPLC-UV) method. An Agilent 1200 series HPLC equipped with an Aglient Eclipse XDB-C18 column, coupled with a G1314B variable wavelength detector was used. The mobile phase was 45% 10 mM phosphate buffer and 55% methanol at a flow rate of 1 mL per minute with a detection wavelength of 234 nm. Under this method, pCBA had a retention time of 7.4 min. All pCBA concentrations utilized in this study were nearly 40 times the estimated PQL of 0.025 mg L^{-1} (Table 5). A sample chromatogram for a 1 mg L^{-1} concentration standard, a typical measured concentration, is shown in Figure 3.

Table 5: Analytical techniques used to quantify concentrations of experimental compounds.

Chemical name	Analytical Techniques	MDL (mg L^{-1})	PQL (mg L^{-1})	RSD at 50 mg L^{-1}
Propylene glycol (PG)	Direct Injection GC-FID	5	25	16%
2-Butoxyethanol (2-BE)	Direct Injection GC-FID	2.5	12.5	10%
Para-chlorobenzoic acid (pCBA)	Direct Injection HPLC-UV	--	0.025	--

GC: gas chromatography; FID: flame ionization detection; HPLC: high performance liquid chromatography; RSD: relative standard deviation

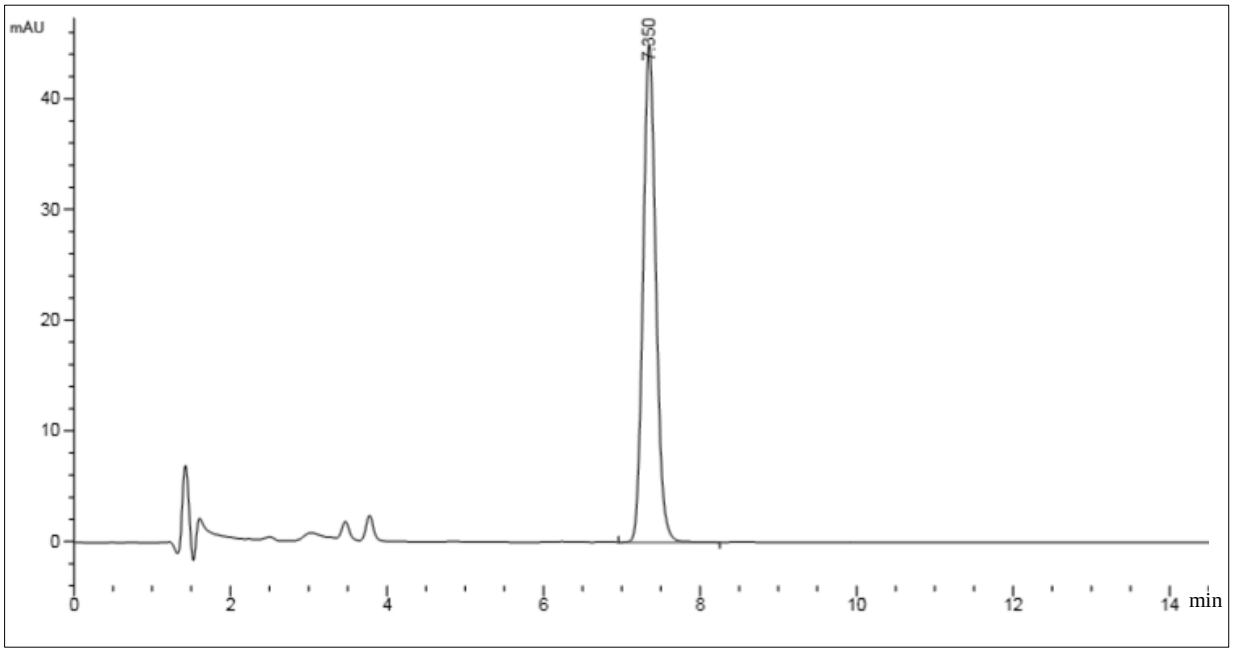

Figure 3: HPLC-UV chromatogram of para-chlorobenzoic acid (pCBA). Example shown is a 1 mg L^{-1} concentration. pCBA retention time is 7.4 min using this previously established method.

3. Results

3.1 Molar absorption coefficients

Molar absorption coefficients were determined for PG and 2-BE and are shown as a function of wavelength in Figure 4. Both PG and 2-BE have compound molar absorption coefficient values greater than zero only at wavelengths less than 270 nm. There is some overlap between the molar absorption coefficient range for 2-BE and the LP and MP UV lamp emissions.

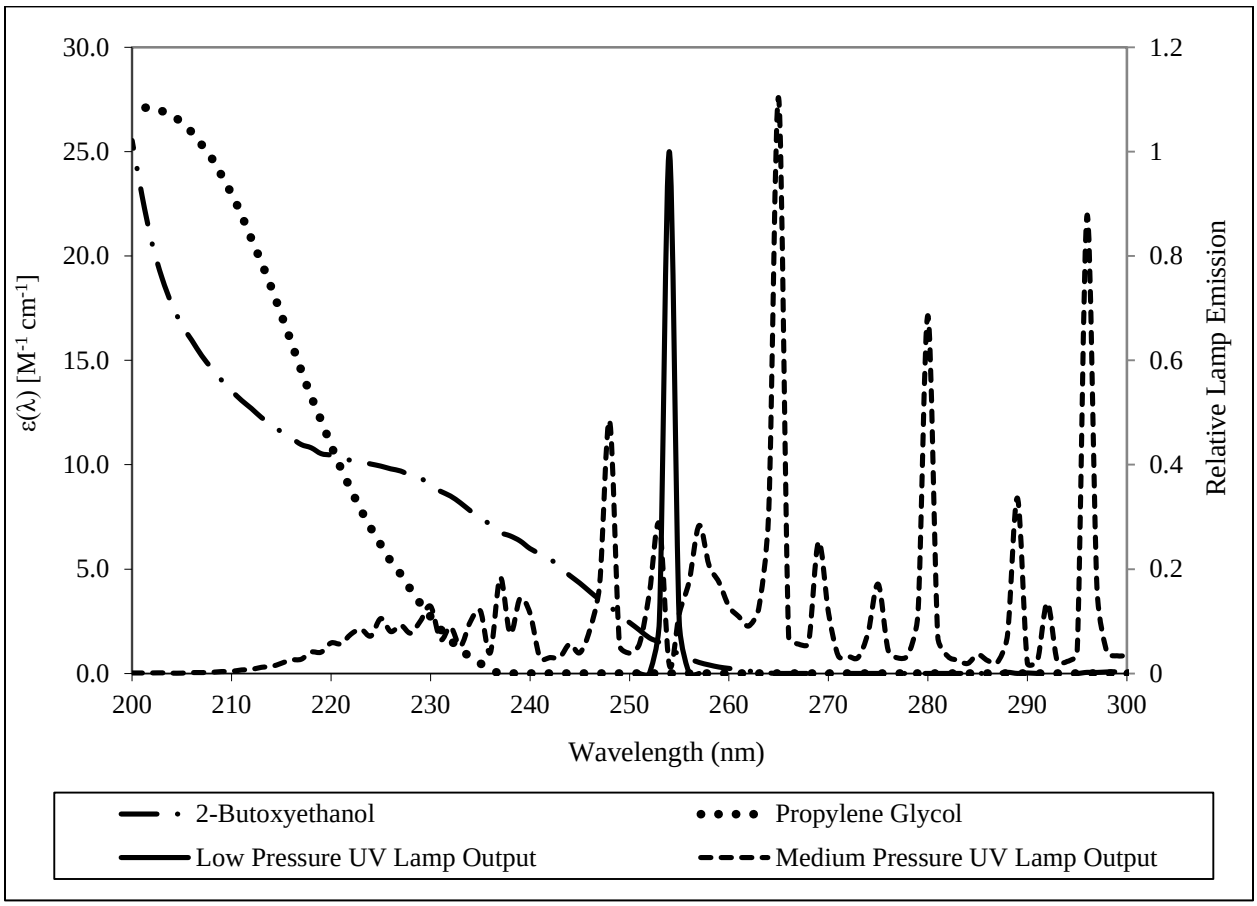

Figure 4: Molar absorption coefficients (ε) for propylene glycol and 2-butoxyethanol as a function of wavelength. UV lamp emission spectrums are presented on the secondary (right) axis and expressed as relative to 254 nm. Overlap between the molar absorption coefficient for 2-BE and the lamp emission suggest 2-BEmay be subject to potential direct photolysis from both LP and MP UV lamps. Direct photolysis of PG is less likely due to nearly non-overlap. These compounds do not have any absorbance features that would be affected by the solar emission spectrum.

3.2 Hydroxyl radical reaction rate constants

This study determined the $k_{HO\bullet}$ to be 6.15×10^8 M^{-1} s^{-1} (± 6%) for PG and 1.15×10^9 M^{-1} s^{-1} (± 4%) for 2-BE (Table 6). These rate constants were determined using Equation 2 and data obtained from competition kinetics experiments. Figure 5 shows the observed changes in peak areas of the target and reference compounds for each experiment as function of UV dose. The observed and direct photolysis rates (k'_{obs} and k'_{d}) used in Equation 2 were determined from the linear regression analysis (95% confidence interval) of these data sets. The reported errors associated with these values are based on the errors attributed to the linear regression. In the PG experiment, neither pCBA nor PG was detected after a 500 mJ cm^{-2} UV dose, as reflected in Figure 5. Direct photolysis was observed for pCBA. No direct photolysis was observed for PG or 2-BE.

Table 6: Hydroxyl radical reaction rate constants ($k_{HO\bullet}$) for propylene glycol and 2-butoxyethanol.

Compound	$k_{HO\bullet}$ [$\times 10^9$ M^{-1} s^{-1}]	Method of Determination	Reference
Propylene glycol (PG)	**0.6 ± 6%**	**Competition Kinetics**	**This Study**
	1.7	Pulse Radiolysis	Buxton *et al.*, 1988
	1.8 ± 0.9	Group Contribution Estimate	Minakata *et al.*, 2009
2-Butoxyethanol (2-BE)	**1.1 ± 4%**	**Competition Kinetics**	**This Study**
	5.3 ± 2.7	Group Contribution Estimate	Minakata *et al.*, 2009

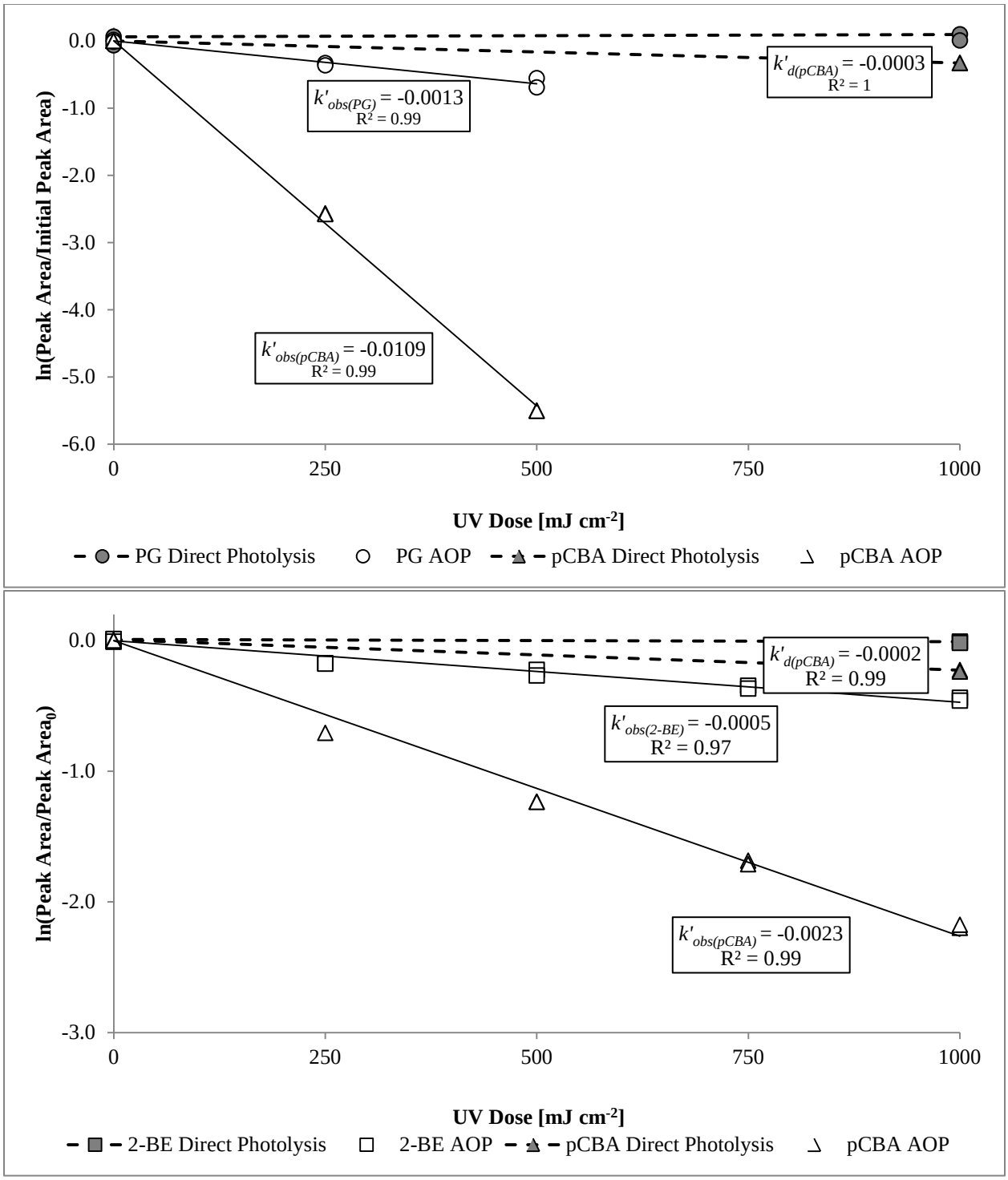

Figure 5: Results of competition kinetics experiments as a function of UV dose. Para-chlorobenzoic acid (pCBA, triangle) was used as the reference compound in both experiments. The TOP graph shows results from the propylene glycol (PG,circle) experiment ($[PG]_0$ = 25 mg L^{-1}, $[pCBA]_0$ = 25 mg L^{-1}). The BOTTOM graph shows the results for the 2-butoxyethanol (2-BE,square) experiment ($[2\text{-BE}]_0$ = 50 mg L^{-1}, $[pCBA]_0$ = 50 mg L^{-1}). Grey data points connected by dashed lines indicate results from direct photolysis experiments to determine k'_d values for each compound, if any. Open data points connected by solid lines indicate results from AOP experiments ($[H_2O_2]_0$ = 50 mg L^{-1}) used to determine k'_{obs} values.

3.3 UV experiments

Low pressure and MP UV experiments conducted in Gulf of Mexico seawater and Boulder Creek surface water samples yielded no significant degradation of either compound with the application of a 2000 mJ cm^{-2} UV dose (Figure 6 and Figure 7). The use of a LP compared to a MP UV system did not impact degradation. Any small changes in concentration witnessed are not statistically significant because they are within the RSD associated with the GC-FID method.

The LP and MP UV/H_2O_2 experiments conducted in ultrapure water resulted in degradation of both PG and 2-BE (Figure 8). Propylene glycol had a reaction rate of $k_{PG} = 2.0 \times 10^{-4}$ mJ^{-1} cm^2 ± 5% for both the LP and MP UV/ H_2O_2 systems. 2-Butoxyethanol reaction rates were slightly faster for the MP UV/H_2O_2 system ($k_{2\text{-}BE,MP} = 9.0 \times 10^{-4}$ mJ^{-1} cm^2 ± 2%) than for the LP UV/H_2O_2 system ($k_{2\text{-}BE,LP} = 5.0 \times 10^{-4}$ mJ^{-1} cm^2 ± 3%). The errors presented represent those associated with the linear regression analysis. No direct photolysis of either compound was observed for the UV doses applied.

Low pressure UV/H_2O_2 experiments conducted in Gulf of Mexico seawater and Boulder Creek surface water samples also resulted in degradation of both target compounds (Figure 9). In the surface water UV/H_2O_2 experiments $k_{PG,surf} = 4.0 \times 10^{-4}$ mJ^{-1} cm^2 ± 3% and $k_{2\text{-}BE,surf} = 5.0 \times 10^{-4}$ mJ^{-1} cm^2 ± 2%. In the seawater UV/H_2O_2 experiments $k_{PG,sea} = 1.0 \times 10^{-4}$ mJ^{-1} cm^2 ± 5% and $k_{2\text{-}BE,sea} = 2.0 \times 10^{-4}$ mJ^{-1} cm^2 ± 3%. The errors presented represent those associated with the linear regression analysis. A more detailed comparison of these values is presented in the Discussion section in Table 7 and Table 8.

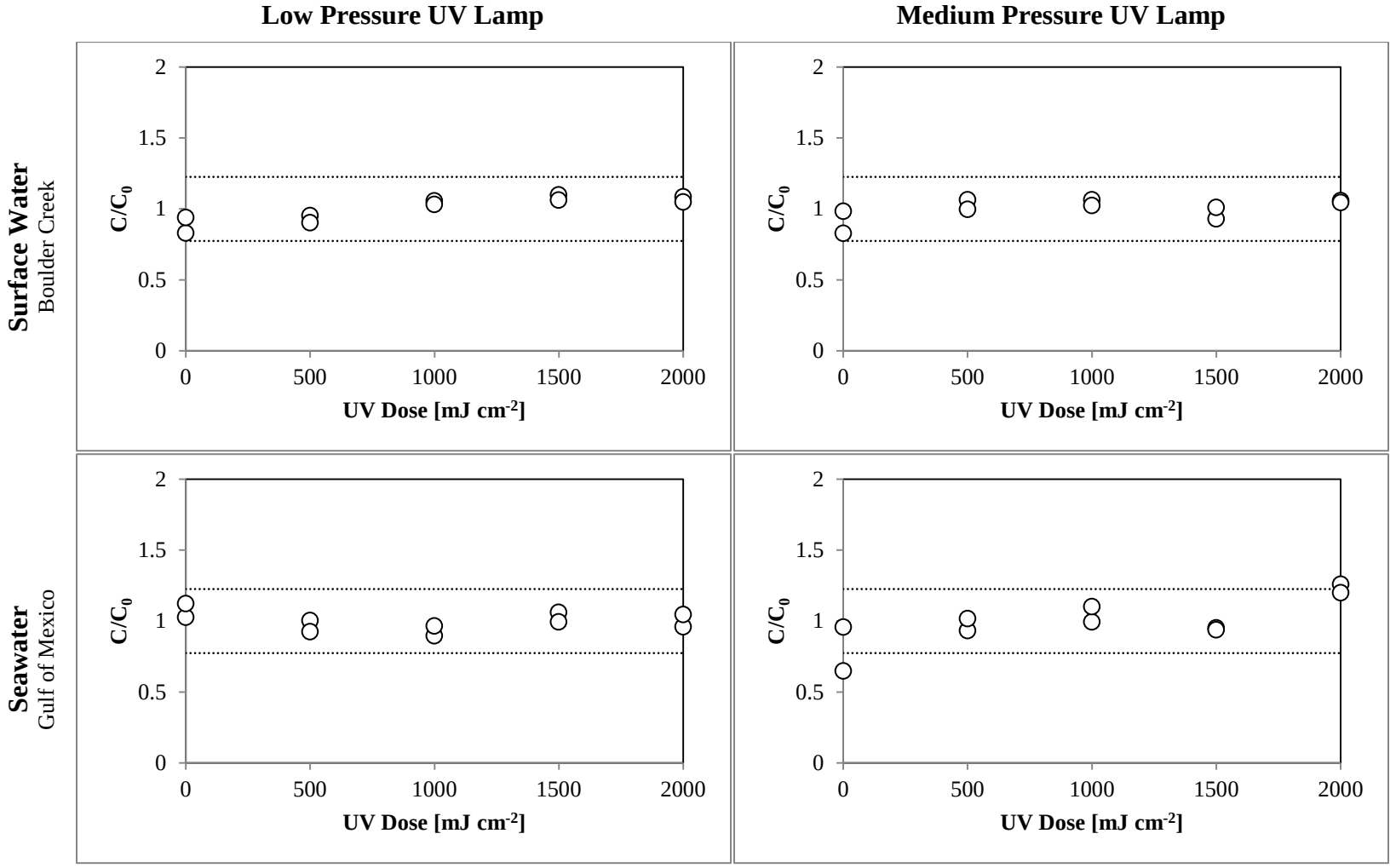

Figure 6: Propylene glycol in natural waters does not significantly degrade with the application of low or medium pressure UV. Individual UV experiments were conducted to assess the indirect photolysis of propylene glycol (circle) in seawater and surface water. Initial compound concentration in all experiments was 50 mg L^{-1}. Error bars represent the 16% RSD due to the GC-FID analytical method and demonstrate that small changes in concentration are not statistically significant.

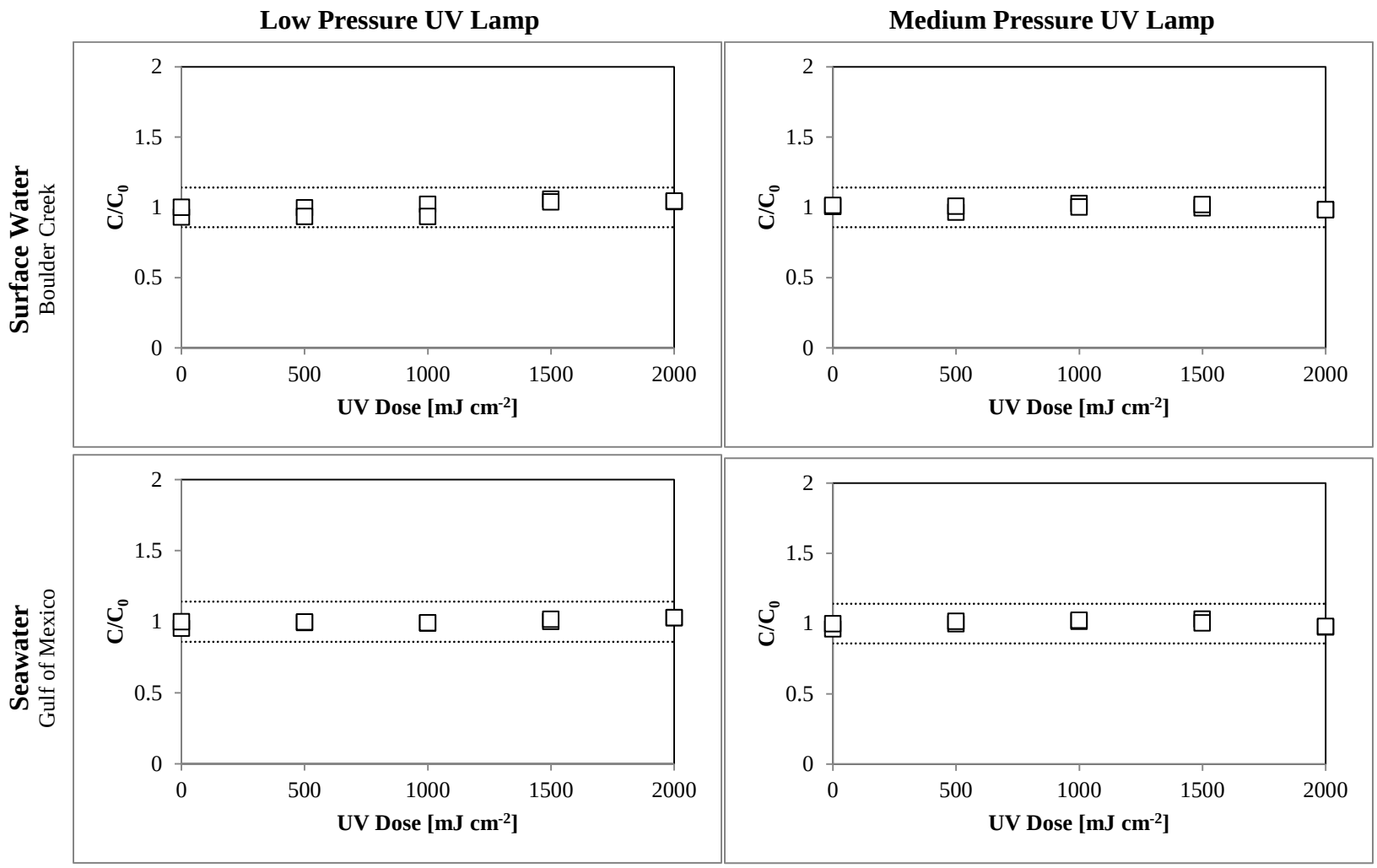

Figure 7: 2-Butoxyethanol in natural waters does not significantly degrade with the application of low or medium pressure UV. Individual UV experiments were conducted to assess the indirect photolysis of 2-butoxyethanol (square) in seawater and surface water. Initial compound concentration in all experiments was 50 mg L^{-1}. Dashed lines represent the 10% RSD due to the GC-FID analytical method and demonstrate that small changes in concentration are not statistically significant.

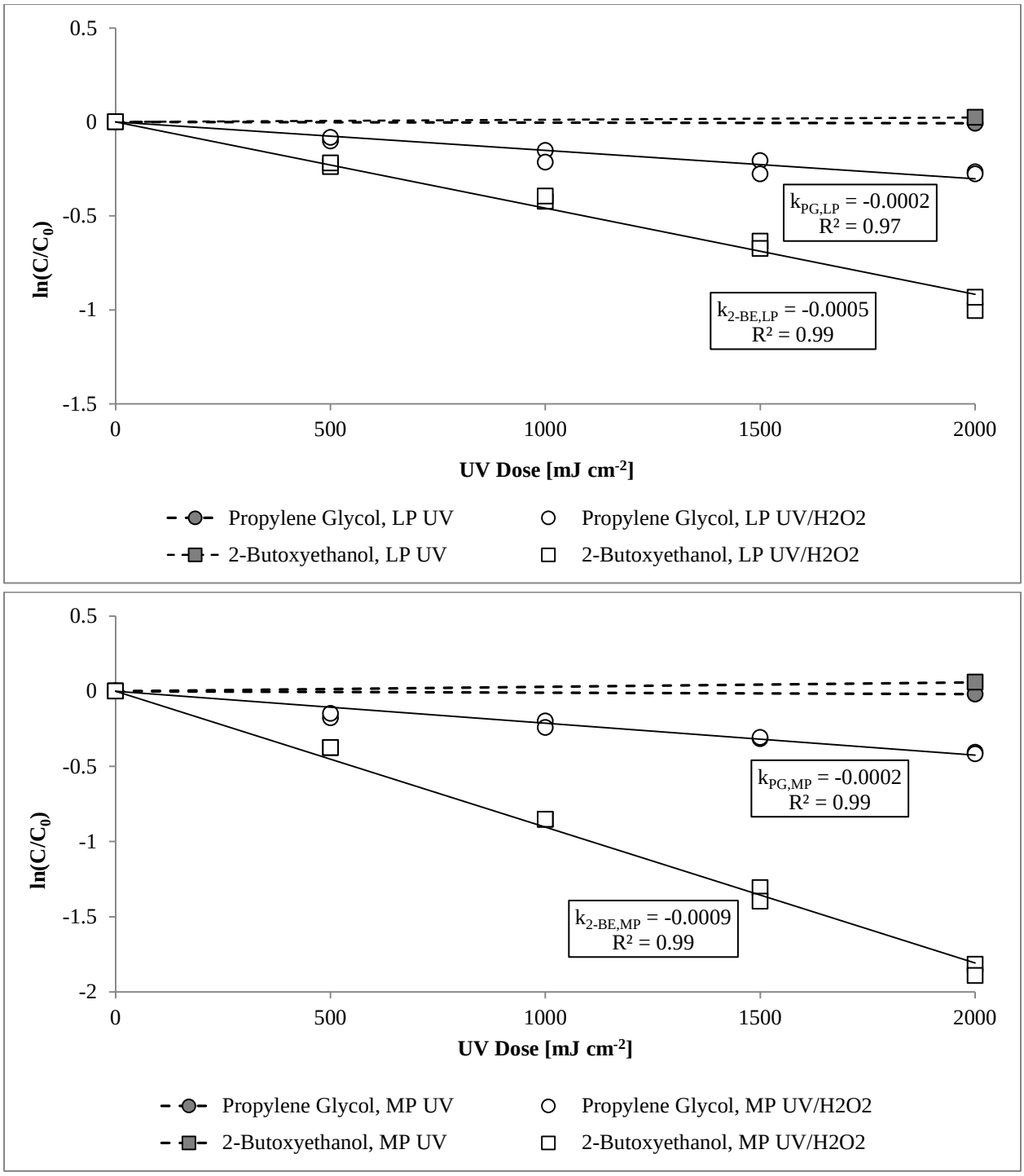

Figure 8: UV/H_2O_2 advanced oxidation processes in ultrapure water degrade propylene glycol (PG, circle**) and 2-butoxyethanol (2-BE,**square**).** Low pressure (top graph) and medium pressure (bottom graph) UV and UV/H_2O_2 experiment results are shown. For all experiments, $[PG]_0$ = 50 mg L^{-1} or $[2\text{-BE}]_0$ = 50mg L^{-1}, respectively. Grey data points connected by dashed lines confirm no significant compound degradation from direct photolysis due to UV application. Open data points connected by solid lines indicate degradation results from AOP experiments ($[H_2O_2]_0$ = 50 mg L^{-1}).

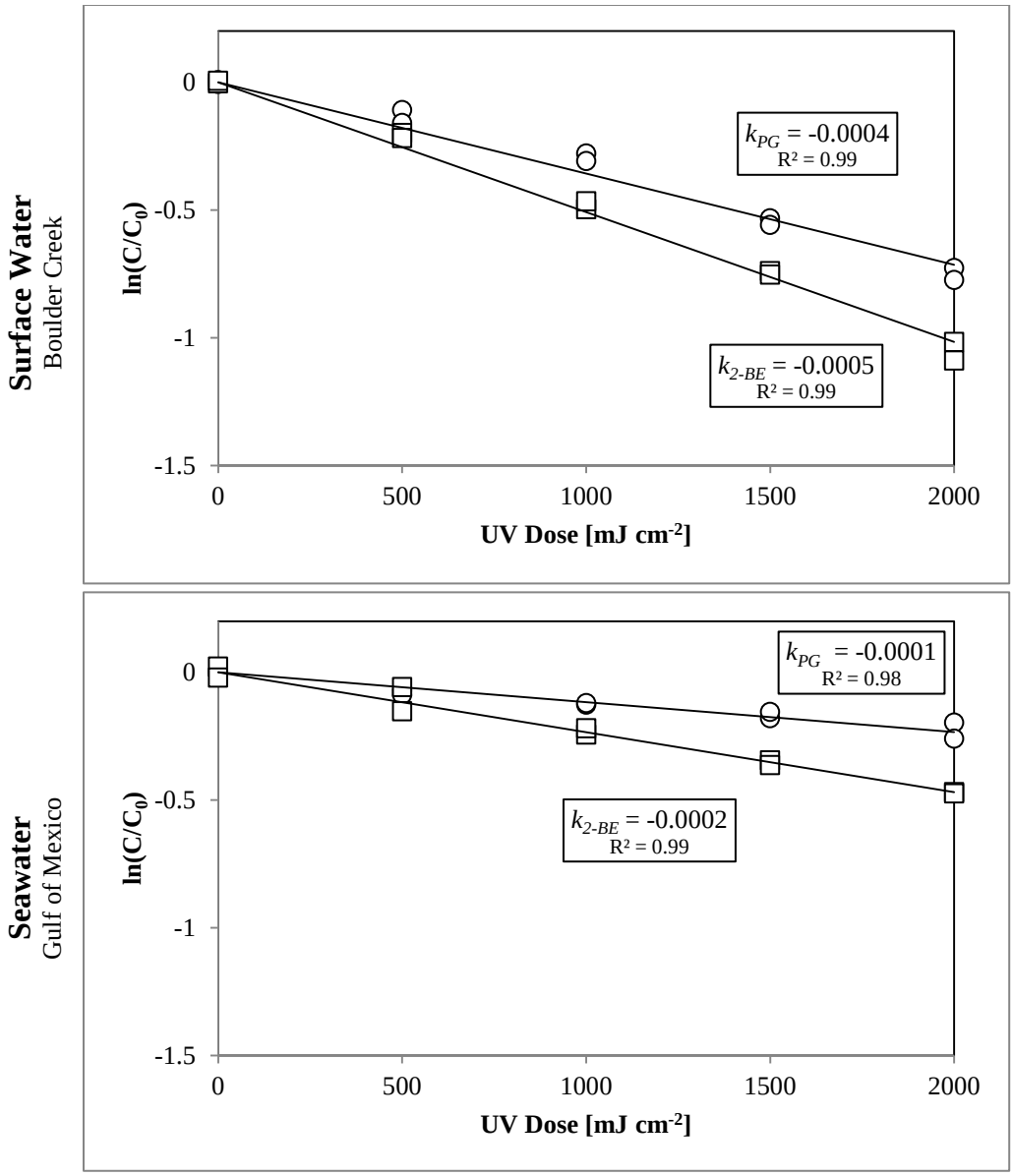

Figure 9: Observed degradation rates of propylene glycol (PG, circle) and 2-butoxyethanol (2-BE, square) in natural waters treated with UV/H_2O_2. Colored data points connected by solid lines indicate degradation results from advanced oxidation process (AOP) experiments ($[H_2O_2]_0$ = 50 mg L^{-1}). Initial compound concentrations were 50 mg L^{-1} in both surface water (top graph) and seawater (bottom graph) scenarios.

3.4 Solar simulation experiments

Degradation due to indirect photolysis was not observed for either compound in solar simulation experiments. No degradation of PG or 2-BE was observed in Gulf of Mexico seawater spiked with initial target compound concentrations of 3.33 mg L^{-1} and irradiated for 7.25 hours. This data is not formally presented because the initial compound concentrations are below the MDLs. Another experiment was conducted, in which ultrapure water was amended with a 0.01 M NO_3^- concentration as a source for $HO^\bullet$ formation. Neither PG nor 2-BE (initial spike concentrations of 0.0005 M) was observed to degrade with over 80 hours of solar simulation (

Figure 10).

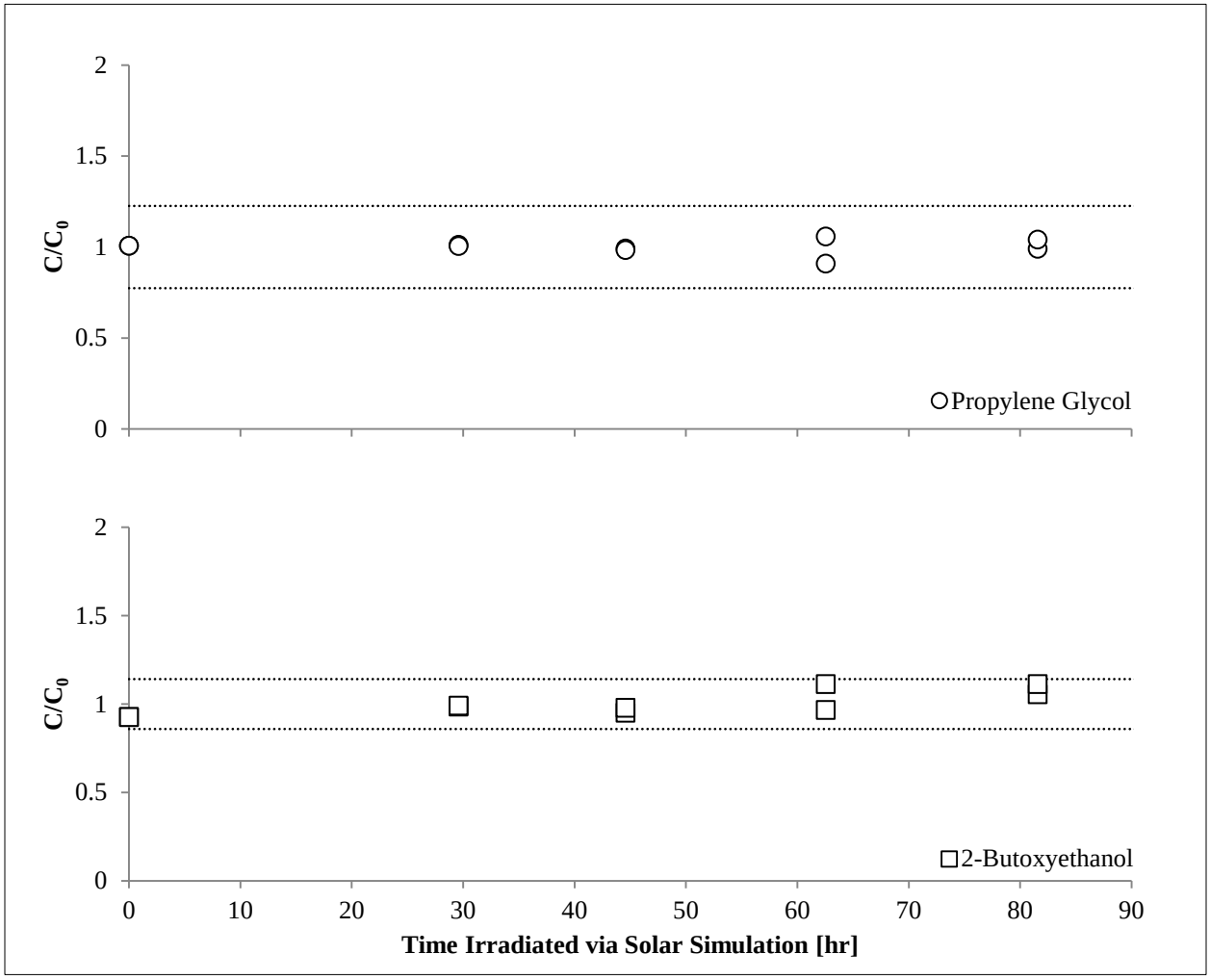

Figure 10: No observed indirect photolysis of propylene glycol (PG, circle) or 2-butoxyethanol (2-BE, square) with solar simulation in nitrate amended solution. Initial experiment concentrations were: $[NO_3^-]$ = 0.01 M, $[PG]_0$ = 0.0005 M, $[2\text{-BE}]_0$ = 0.0005 M. The dashed lines represent the RSD of the GC-FID analytical method (16% for PG and 10% for 2-BE) and emphasize that any small observed changes in concentration are not statistically significant.

4. Discussion

4.1 Molar absorption coefficients and direct photolysis potential

Significant direct photolysis of either PG or 2-BE from sunlight is unlikely. Compound molar absorption coefficient values are greater than zero only at wavelengths less than 270 nm (Figure 4); solar emissions on the earth surface that can impact direct photolysis typically range from 280 nm to 400 nm (

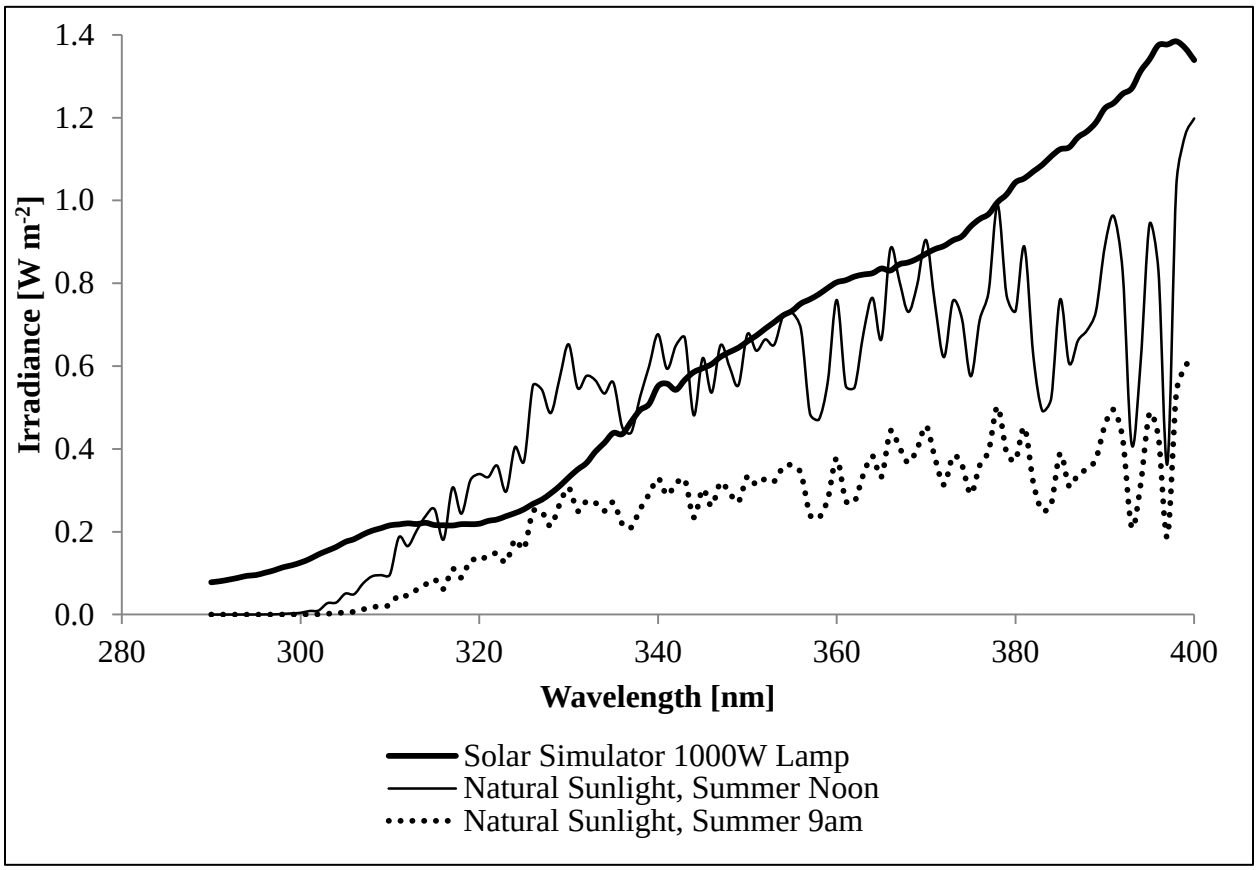

Figure 1), above the wavelength absorption ranges of the compounds.

For LP and MP UV lamp systems direct photolysis could potentially contribute to compound degradation. Overlap between the molar absorption coefficient range for 2-BE and the lamp emission suggest 2-BE may be subject to potential direct photolysis from both LP and MP UV lamps. Direct photolysis of PG is less likely due to nearly non-overlap, yet may be affected

by MP UV lamps (Figure 4). Also, if either of the compounds had high quantum yields, they may degrade despite low absorption. The insignificance of direct photolysis to overall compound degradation was confirmed by the UV experiments conducted in ultrapure water. No degradation was observed when compounds were spiked into ultrapure water and exposed to LP and MP UV doses up to 2000 mJ cm^{-2} (Figure 8), suggesting that these compounds also have low quantum yields.

4.2 Comparison of experimental and estimated k_{HO}. values

Hydroxyl radical reaction rate constants determined in this research using competition kinetics compare well with estimates using the group contribution method established by Minakata *et al.* (2009). These values are presented in Table 6 and a graphical comparison is shown in Figure 11. According to Minakata *et al.*, k_{HO}. values estimated using the group contribution method should fall within 0.5 – 2 times the experimental k_{HO}.. Alternatively, the estimated k_{HO}. values can be said to have an associated RSD of 50%. Although the results from this study are not directly within the expected range of values from the group contribution method, they are very near to it. When compared to the experimentally determined PG value, the group contribution method median estimate has an error of 200%; the group contribution method low end estimate has an error of 50%. When compared to the experimentally determined 2-BE value, the group contribution method median estimate has an error of 380%; the group contribution method low end estimate has an error of 135%. Given the inherent experimental uncertainties associated with performing competition kinetics experiments, combined with the roughness of the uncertainties presented with the model, the experimental and estimated values align well.

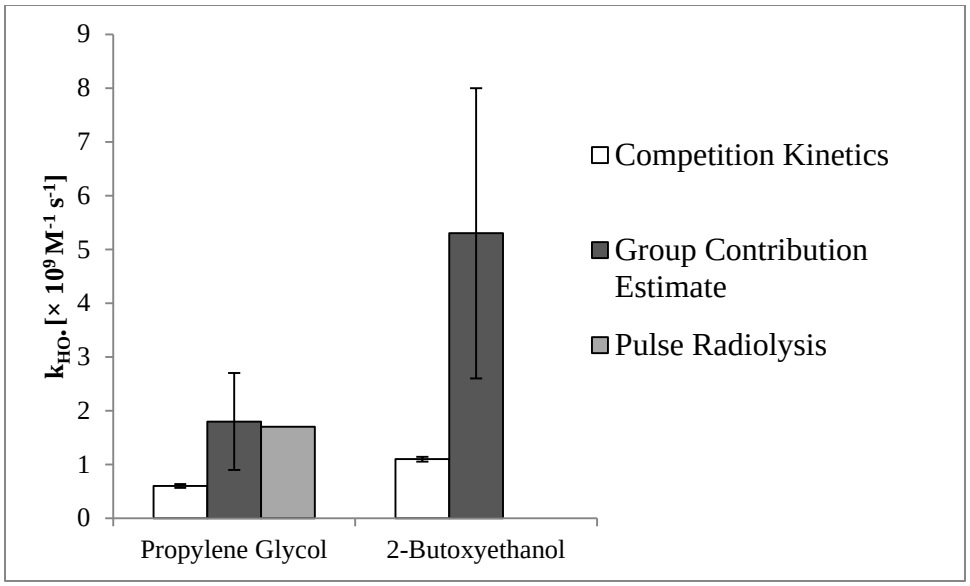

Figure 11: Comparison of hydroxyl radical reaction rate constants ($k_{HO\cdot}$) obtained experimentally and estimated using a group contribution method. The error bars on the data obtained by competition kinetics experiments represents the error associated with the linear regression. The error bars on the group contribution method estimated values represents the model creator's witnessed typical error of the model.

A previously published $k_{HO\cdot}$ value for PG exists. This value, 1.7×10^9 M^{-1} s^{-1}, was determined using pulse radiolysis (Buxton *et al.* 1988). The consistency of the published pulse radiolysis value for PG and the value estimated using the group contribution method (1.7×10^9 M^{-1} s^{-1} vs. $1.8 \pm 0.9 \times 10^9$ M^{-1} s^{-1}, respectively) is most likely due to the usage of the previously published value in the calibration and development of the group contribution method. Therefore, this inherent alignment would be expected and does not signify that the results obtained in this study are inaccurate.

4.3 Implications of Solar Simulation, UV, and UV/AOP experiment results

PG and 2-BE are effectively degraded through indirect photolysis in the presence of high $[HO^{\bullet}]_{ss}$, as witnessed in the UV/H_2O_2 experiments conducted in this study ($[HO^{\bullet}]_{ss} = 4.1 \times 10^{-14}$ M to 2.6×10^{-13} M). These results suggest that UV/AOP such as UV/H_2O_2 are feasible alternatives for the treatment of waters or wastes containing PG and/or 2-BE.

The degradation rates of the compounds in seawater and surface water LP UV/H_2O_2 experiments differ from those witnessed in the ultrapure water LP UV/H_2O_2 experiments despite similar experimental parameters such as initial target compound concentrations, UV dose, and H_2O_2. It is expected that all experimental systems should have nearly the same $[HO^{\bullet}]_{ss}$ and that target compound degradation rates should not be statistically different. Statistical differences in the degradation rates were analyzed using single factor ANOVA analysis paired with a 2-tailed student's t-test for individual comparisons ($\alpha = 0.005$). The degradation rates of PG in ultrapure water and seawater were not statistically different yet both were statistically different from the degradation rate in surface water (Table 7). The degradation rates of 2-BE in ultrapure water and surface water were not statistically different, but both were statistically different from the degradation rate in seawater (Table 8).

Table 7: Statistical significance of observed differences in propylene glycol degradation with LP UV/H_2O_2 in varying matrices. The degradation rates (k) were compared using a 2-tailed student's t-test ($\alpha = 0.005$). A "No" indicates that the values are not statistically different.

	Matrix and k [$\times 10^{-4}$ mJ^{-1} cm^2]			
Matrix and k [$\times 10^{-4}$ mJ^{-1} cm^2]	**Propylene Glycol**	Ultrapure 2.0	Surface Water 4.0	Seawater 1.0
	Ultrapure 2.0	--	Yes	No
	Surface Water 4.0	Yes	--	Yes
	Seawater 1.0	No	Yes	--

Table 8: Statistical significance of observed differences in 2-butoxyethanol degradation with LP UV/H_2O_2 in varying matrices. The degradation rates (k) were compared using a 2-tailed student's t-test ($\alpha = 0.005$). A "No" indicates that the values are not statistically different.

	Matrix and k [× 10^{-4} mJ^{-1} cm^2]			
Matrix and k [× 10^{-4} mJ^{-1} cm^2]	**2-Butoxy-ethanol**	Ultrapure 5.0	Surface Water 5.0	Seawater 2.0
	Ultrapure 5.0	--	No	Yes
	Surface Water 5.0	No	--	Yes
	Seawater 2.0	Yes	Yes	--

For the LP UV/H_2O_2 experiments, the expected first-order degradation rates were modeled based on the $[HO^{\bullet}]_{ss}$ of the system. Model parameters included incident irradiance, sample depth, sample absorbance at 254 nm, pH, DOC, alkalinity, inherent $HO^{\bullet}$ photoproduction rate of the water, initial H_2O_2 concentration, and initial target compound concentration. The models are shown overlaid with the experimental data points for PG in Figure 12 and 2-BE in Figure 13. The lack of significant variation in the modeled degradation rates illustrates that the UV/H_2O_2 process is the controlling factor and that the water matrix has little impact on overall degradation. For PG, the seawater experimental data aligns especially well with the modeled predictions. The seawater, ultrapure water, and surface water modeled rates are 20%, 60%, and 80% less than the experimentally obtained rates. For 2-BE, the seawater experimental data aligns best with the modeled predictions. The seawater, ultrapure water, and surface water modeled rates are 50%, 80%, and 80% less than the experimentally obtained rates.

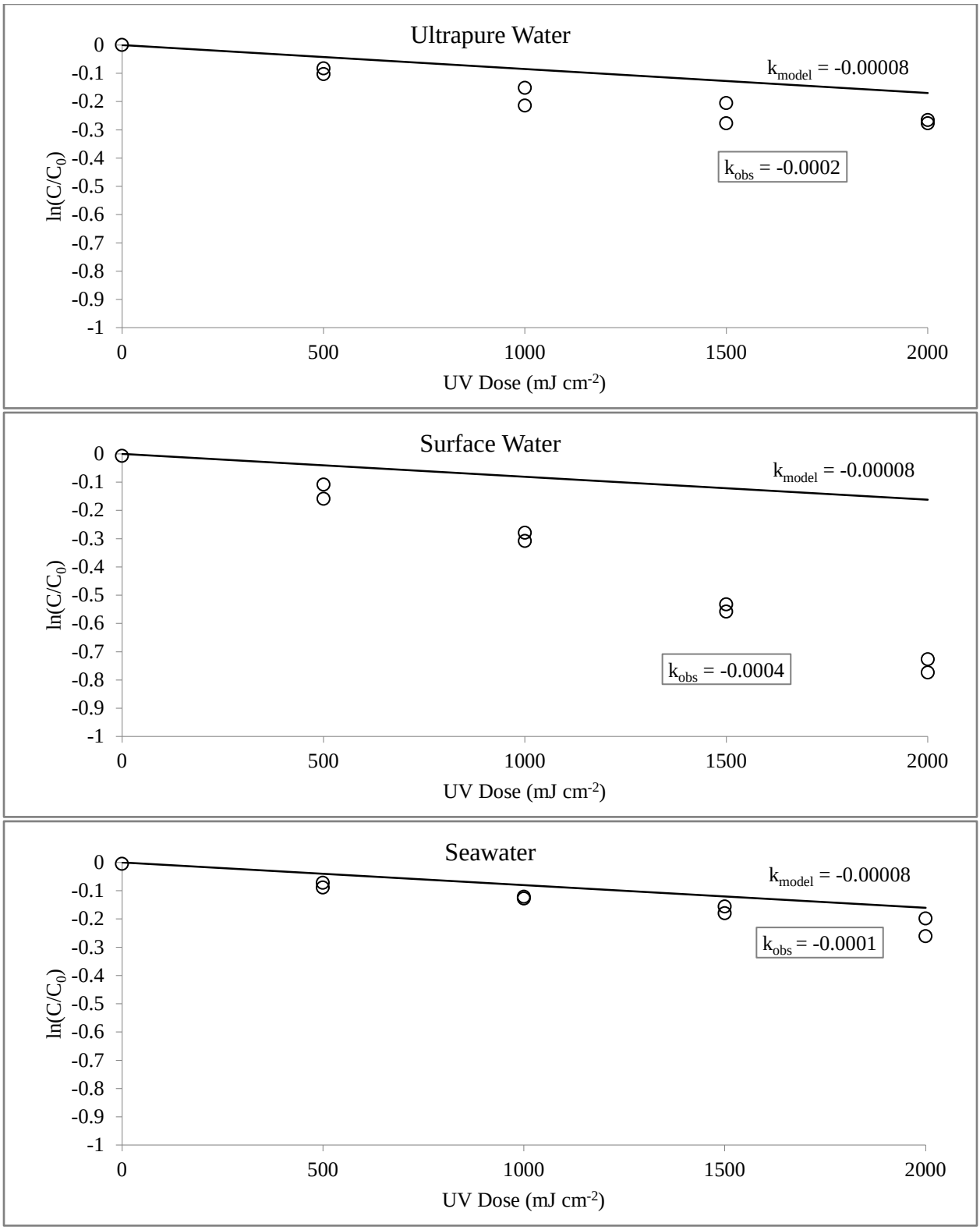

Figure 12: Comparison of modeled decay and experimental data points for PG in three different matrices. The solid lines are the modeled degradation. The circle data points are the experimentally observed degradation. The experiments modeled and conducted were for LP UV/AOP ($[PG]_0$ = 50 mg L^{-1}, $[H_2O_2]_0$ = 50 mg L^{-1}).

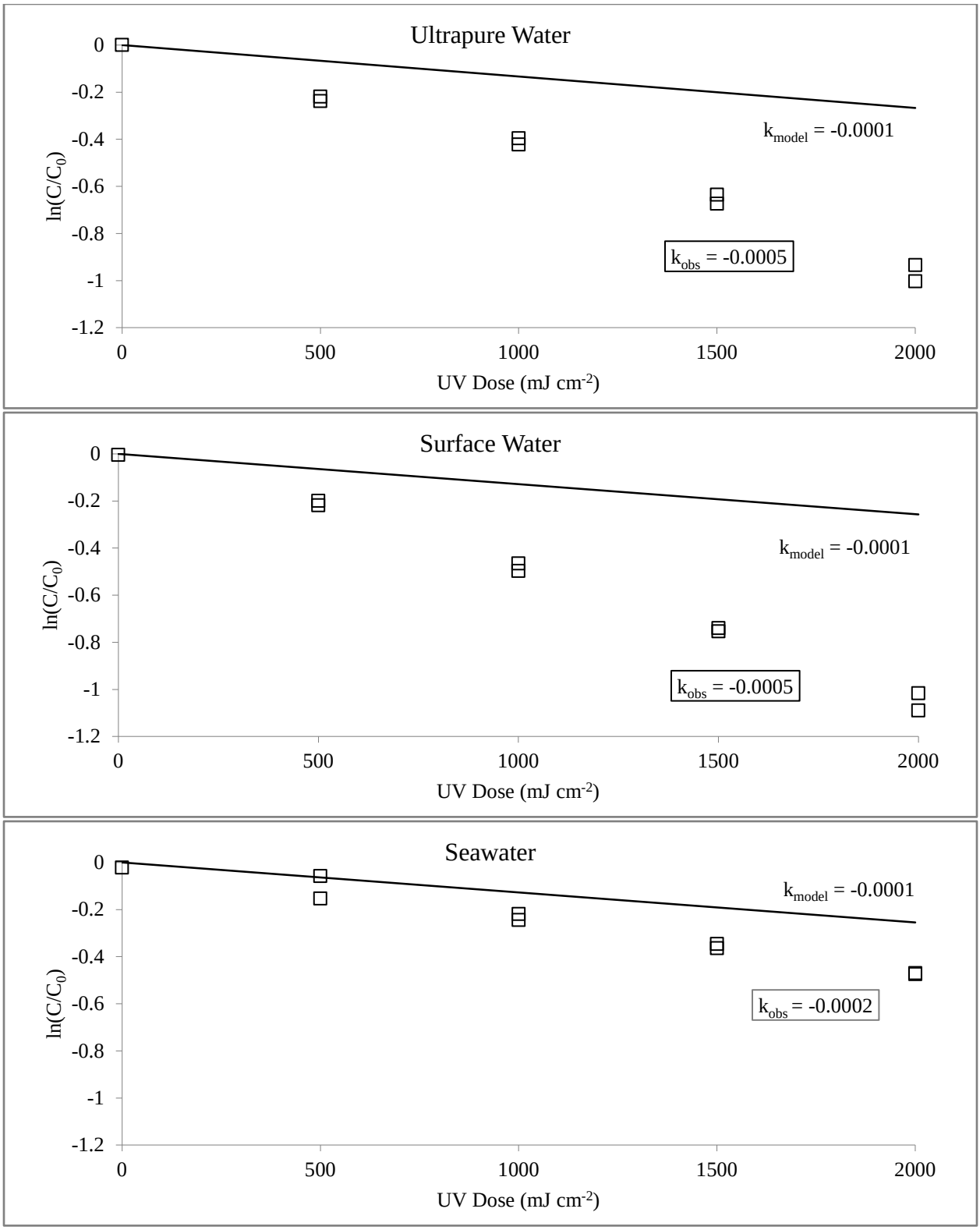

Figure 13: Comparison of modeled decay and experimental data points for 2-BE in three different matrices. The solid lines are the modeled degradation. The square data points are the experimentally observed degradation. The experiments modeled and conducted were for LP UV/AOP ($[2\text{-BE}]_0$ = 50 mg L^{-1}, $[H_2O_2]_0$ = 50 mg L^{-1}).

In natural systems, neither PG nor 2-BE is expected to undergo significant, rapid degradation due to direct or indirect photolysis. The UV surface water experiments had calculated $[HO^{\bullet}]_{ss}$ ranging from 3.2×10^{-17} M to 3.8×10^{-17} M. The solar simulation and UV seawater experiments had calculated $[HO^{\bullet}]_{ss}$ ranging from 2.7×10^{-18} M to 5.8×10^{-18} M. These experimental $[HO^{\bullet}]_{ss}$ are reflective of those encountered in natural waters. Reported $[HO^{\bullet}]_{ss}$ in natural waters including rivers and lakes range from 2.0×10^{-17} M to 9.9×10^{-16} M (Vione *et al.* 2010, Brezonik and Fulkerson-Brekken 1998, Haag and Hoigne 1985). Reported $[HO^{\bullet}]_{ss}$ in seawater samples range from 3.1×10^{-20} M to 3.0×10^{-17} M (Mopper and Zhou 1990, Qian *et al.* 2001, Zepp *et al.* 1987, Takeda *et al.* 2004, Arakaki *et al.* 2010) (Appendix A). Due to the lack of observed direct and indirect photolysis in these experiments, rapid photodegradation of either PG or 2-BE during in natural systems appears unlikely, especially in an oil spill response scenario. The Corexit dispersants have been demonstrated to achieve 90%-100% oil dispersion within 30 minutes of application (Belore, 1999). Dispersant compounds including PG and 2-BE can therefore conservatively be expected to only be in the surface of the water column where they may undergo photodegradation processes for less than 30 minutes. Log removal vs. concentration – time (Ct) models were created for each compound based on the experimentally obtained hydroxyl radical reaction rates. The modeling equation is presented below.

Equation 4: Determining percent removal of a compound as a function of $[HO^{\bullet}]_{ss}$ and time. $k_{HO\bullet}$ is the hydroxyl radical reaction rate of the compound.

$$\frac{Percent\ Removal\ (\%)}{100} = 1 - e^{k_{HO\bullet}[HO\bullet]_{ss}t}$$

Ct is expressed as $[HO^{\bullet}]_{ss}$ multiplied by exposure time to that $[HO^{\bullet}]_{ss}$. This model is presented graphically in Figure 14. Experimental data sets are plotted against the model to show that the model conservative with respect to degradation rate. This model can be used to predict the time

required to achieve a desired removal of the compounds. For example, to achieve a 5% removal of PG or 2-BE in a seawater with a typical $[HO^{\bullet}]_{ss}$ of 10^{-18} M, the compounds would need to be exposed to this $[HO^{\bullet}]_{ss}$ for 2.7 and 1.5 years, respectively. This timeframe is obviously much longer than the 30 minutes of anticipated exposure time.

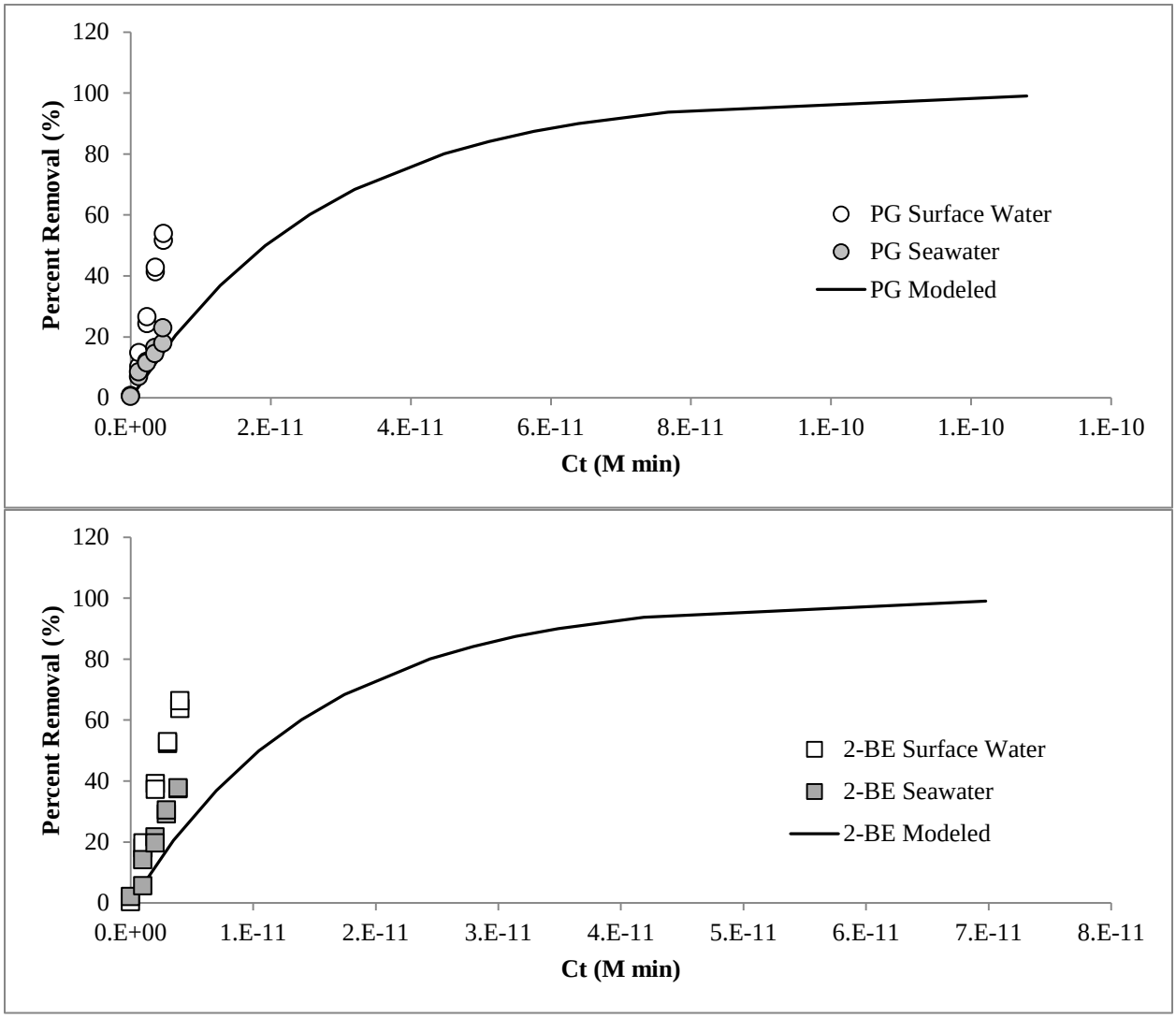

Figure 14: Percent removal as a function of $[HO^{\bullet}]_{ss}$ and exposure time (Ct). PG is shown in the top graph, 2-BE in the bottom graph. The solid lines are the modeled percent removal based on the experimentally obtained hydroxyl radical reaction rate constants for the compounds. The square data points are experimentally observed degradation.

Although solar simulation experiments in seawater and NO_3^- amended waters showed degradation of PG and 2-BE by direct or indirect photolysis to be insignificant, this does not imply that the compounds are likely to persist in the open ocean if dispersants are applied as part of an oil spill response. It is important to note that both PG and 2-BE have been shown to be readily biodegraded. West *et al.* found that PG degraded in seawater with a half-life of 13.6 days (Table 2) (West *et al.* 2007). 2-Butoxyethanol has a reported half-life in surface water of 7-28 days (ATSDR 1998). Long-term persistence of these compounds should only be a concern in waters in which biologically activity is severely limited. Possible biologically limited scenarios may include some oil spills in which biodegradation is inhibited due to competition kinetics or toxicity effects.

After the Deepwater Horizon Blowout, studies were conducted to assess the fate and transport of the constituents of the Corexit dispersants. Dilution alone has been shown to effectively reduce dispersant compound concentrations in the open ocean. Kujawinski *et al.* observed that detected concentrations of DOSS during and immediately following Corexit application decreased due to dilution and turbulent mixing. An example of the observed concentration gradient is a drop from 7-12 ppb DOSS at the wellhead to 0.04 ppb DOSS at a 300km distance (Kujawinski *et al.* 2011). A sampling effort conducted by the Operational Science Advisory Team used PG, 2-BE, DOSS, and DPnB as markers to determine Corexit concentrations in the Gulf of Mexico. Seawater samples were collected from nearshore (4,850 samples), offshore (440 samples), and deep water locations (4,114) during the 5 month period immediately following initial dispersant application. None of the 9,404 collected samples contained Corexit compounds at concentrations above the EPA benchmarks for aquatic life (2010). Hayworth and Clement detected PG, 2-BE, and DOSS in nearshore and inland Gulf

Coast water samples collected 2-6 months post-Corexit application, yet these detections were ultimately attributed to stormwater discharge (2012).

The lack of observed photochemical degradation of PG and 2-BE in natural waters demonstrates the stability of these compounds. In dispersant formulations, stable compounds which will not rapidly photodegrade upon surface application are desirable. The results of this research suggest that solar exposure will not reduce the operational efficiency of a dispersant with respect to the solvent constituents PG and 2-BE. Yet, many unknown complexities of oil-dispersant mixtures have yet to be explored. Indirect photolysis of PG and 2-BE does become a significant driver of overall degradation in systems with high $[HO^{\bullet}]_{ss}$, as shown by the observed degradation in the engineered UV/H_2O_2 experiments. These experiments had $[HO^{\bullet}]_{ss}$ of 4.1×10^{-14} M to 2.6×10^{-13} M. And, studies have shown that higher concentrations of reactive oxygen species such as $HO^{\bullet}$ may be present in a spill scenario. Crude oil has been shown to be a source for reactive oxygen species such as singlet oxygen (Correa *et al.* 2012) and $HO^{\bullet}$ (Appendix B). If the formation of $HO^{\bullet}$ from oil is high enough to provide a $[HO^{\bullet}]_{ss} > 10^{-14}$ M, photo-induced degradation of PG and 2-BE may be similar to the rapid compound loss witnessed in the UV/ H_2O_2 experiments. Further investigation of oil-dispersant interactions with regards to photodegradation is warranted before comprehensive conclusions regarding the stability of dispersant compounds can be made.

References

Arakaki, T., Hamdun, A., Uehara, M. and Okada, K. (2010) Photochemical Formation of Hydroxyl Radicals in Red Soil-Polluted Seawater on the North of Okinawa Island, Japan. *Water Air and Soil Pollution* 209(1-4), 191-198.

ATSDR (1997) Toxicological Profile for Propylene Glycol.

ATSDR (1998) Toxicological Profile for 2-Butoxyethanol and 2-Butoxyethanol Acetate.

Bausmith, D.S. and Neufeld, R.D. (1999) Soil biodegradation of propylene glycol based aircraft deicing fluids. *Water Environment Research* 71(4), 459-464.

Belore, Randy (1999). Wave tank tests to determine the effectiveness of Corexit 9500 dispersant on Hibernia crude oil under cold water conditions. *Artic and Marine Oil Spill Program Technical Seminar* 2, 35-740. Environment Canada.

Bolton, J.R. and Linden, K.G. (2003) Standardization of methods for fluence (UV dose) determination in bench-scale UV experiments. *Journal of Environmental Engineering-Asce* 129(3), 209-215.

Brezonik, P.L. and Fulkerson-Brekken, J. (1998) Nitrate-induced photolysis in natural waters: Controls on concentrations of hydroxyl radical photo-intermediates by natural scavenging agents. *Environmental Science & Technology* 32(19), 3004-3010.

Buxton, G.V., Greenstock, C.L., Helman, W.P. and Ross, A.B. (1988) Critical review of rate constants for reactions of hydrated electrons, hdrogen-atoms and hydroxyl radicals in aqueous solution. *Journal of Physical and Chemical Reference Data* 17(2), 513-886.

Castro, S., Davis, L.C. and Erickson, L.E. (2001) Plant-enhanced remediation of glycol-based aircraft deicing fluids, pp. 141-152, Practice Periodical of Hazardous, Toxic, and Radioactive Waste Management.

Correa, R.J., Severino, D., Souza, R.D., de Santana, E.F., Mauro, L.L., Alvarenga, S.D.S. and Nicodem, D.E. (2012) The generation of singlet oxygen by petroleum and its fractions. *Journal of Photochemistry and Photobiology a-Chemistry* 236, 9-13.

Corsi, S.R., Booth, N.L. and Hall, D.W. (2001) Aircraft and runway deicers at General Mitchell International Airport, Milwaukee, Wisconsin, USA. 1. Biochemical oxygen demand and dissolved oxygen in receiving streams. *Environmental Toxicology and Chemistry* 20(7), 1474-1482.

Dong, M.M. and Rosario-Ortiz, F.L. (2012) Photochemical Formation of Hydroxyl Radical from Effluent Organic Matter. *Environmental Science & Technology* 46(7), 3788-3794.

Elovitz, M.S. and von Gunten, U. (1999) Hydroxyl radical ozone ratios during ozonation processes. I-The R-ct concept. *Ozone-Science & Engineering* 21(3), 239-260.

EPA (2010) Questions and answers on dispersants. EPA Response to BP Oil Spill in the Gulf of Mexico.

European Centre for Ecotoxicology and Toxicology. (1994) Butoxyethanol Criteria Document: Including a Supplement for 2-Butoxyethyl Acetate.

Haag, W.R. and Hoigne, J. (1985) Photo-sensitized oxidation in natural-water via OH radicals. *Chemosphere* 14(11-12), 1659-1671.

Hayworth, J.S. and Clement, T.P. (2012) Provenance of Corexit-related chemical constituents found in nearshore and inland Gulf Coast waters. *Marine Pollution Bulletin* 64(10), 2005-2014.

Jaesche, P., Totsche, K.U. and Kogel-Knabner, I. (2006) Transport and anaerobic biodegradation of propylene glycol in gravel-rich soil materials. *Journal of Contaminant Hydrology* 85(3-4), 271-286.

Klassen, N.V., Marchington, D. and McGowan, H.C.E. (1994) H2O2 determination by the I-3(-) method at by KMNO4 titration. *Analytical Chemistry* 66(18), 2921-2925.

Klecka, G.M., Carpenter, C.L. and Landenberger, B.D. (1993) Biodegradatio of aircraft deicing fluids in soil at low temperatures. *Ecotoxicology and Environmental Safety* 25(3), 280-295.

Kujawinski, E.B., Soule, M.C.K., Valentine, D.L., Boysen, A.K., Longnecker, K. and Redmond, M.C. (2011) Fate of Dispersants Associated with the Deepwater Horizon Oil Spill. *Environmental Science & Technology* 45(4), 1298-1306.

McPherson, A.K., Gill, A.C. and Moreland, R.S. (2005) Assessment of water quality, benthic invertebrates, and periphyton in the Threemile Creek basin, Mobile, Alabama, p. 153, USGS.

Minakata, D., Li, K., Westerhoff, P. and Crittenden, J. (2009) Development of a Group Contribution Method To Predict Aqueous Phase Hydroxyl Radical (HO center dot) Reaction Rate Constants. *Environmental Science & Technology* 43(16), 6220-6227.

Mopper, K. and Zhou, X.L. (1990) Hydroxyl radical photoproduction in the sea and its potential impact on marine processes. *Science* 250(4981), 661-664.

Qian, J.G., Mopper, K. and Kieber, D.J. (2001) Photochemical production of the hydroxyl radical in Antarctic waters. *Deep-Sea Research Part I*-Oceanographic Research Papers 48(3), 741-759.

Shemer, H., Sharpless, C.M., Elovitz, M.S. and Linden, K.G. (2006) Relative rate constants of contaminant candidate list pesticides with hydroxyl radicals. *Environmental Science & Technology* 40(14), 4460-4466.

Schoenberg, T., Veltman, S. and Switzenbaum, M. (2001) Kinetics of anaerobic degradation of glycol-based Type I aircraft deicing fluids. *Biodegradation* 12(1), 59-68.

Schwarzenbach, R.P., Gschwend, P.M. and Imboden, D.M. (1993) Environmental Organic Chemistry, John Wiley & Sons, Inc., Honoken, New Jersey.

Takeda, K., Takedoi, H., Yamaji, S., Ohta, K. and Sakugawa, H. (2004) Determination of hydroxyl radical photoproduction rates in natural waters. *Analytical Sciences* 20(1), 153-158.

Team, O.S.A. (2010) Summary Report for Sub-sea and Sub-surface Oil and Dispersant Detection: Sampling and Monitoring, p. 131, OSAT, Unified Area Command, New Orleans, LA.

Veltman, S., Schoenberg, T. and Switzenbaum, M.S. (1998) Alcohol and acid formation during the anaerobic decomposition of propylene glycol under methanogenic conditions. *Biodegradation* 9(2), 113-118.

Vione, D., Bagnus, D., Maurino, V. and Minero, C. (2010) Quantification of singlet oxygen and hydroxyl radicals upon UV irradiation of surface water. *Environmental Chemistry Letters* 8(2), 193-198.

West, R.J., Davis, J.W., Pottenger, L.H., Banton, M.I. and Graham, C. (2007) Biodegradability relationships among propylene glycol substances in the organization for economic cooperation and development ready- and seawater biodegradability tests. *Environmental Toxicology and Chemistry* 26(5), 862-871.

Yasuhara, A., Shiraishi, H., Tsuji, M. and Okuno, T. (1981) Analysis of organic-substances in highly polluted river water by mass-spectrometry. *Environmental Science & Technology* 15(5), 570-573.

Zepp, R.G., Hoigne, J. and Bader, H. (1987) Nitrate-induced photooxidation of trace organic-chemicals in water. *Environmental Science & Technology* 21(5), 443-450.

Appendix A

Reported Hydroxyl Radical Steady State Concentrations in Natural Waters

Table A-1: Reported $HO^{\bullet}$ Steady State Concentrations, Formation Rates, and Source Contributions in Seawaters of Varying Type and Depth

Sample Description	$[HO^{\bullet}]_{ss}$ $\times 10^{-18}$ M	$HO^{\bullet}$ formation rate $\times 10^{-12}$ M s^{-1}	$HO^{\bullet}$ formation from different sources (%)					Probe Method	Reference
			NO_3^-	NO_2^-	H_2O_2	Fenton	Other (DOM)		
Surface Waters									
Open-ocean									
Pacific Ocean	0.22		100					estimated	Zepp *et al.* (1987)
Sargasso Sea	1.1 ± 0.1	2.8 ± 0.2	<1	ND	<4		>95	methanol	Mopper & Zhou (1990)
Gulf Stream	1.2	3.1						methanol	Mopper & Zhou (1990)
Crystal Sound, Antarctica	2.8	0.34	~33	67			67	benzoic acid	Qian *et al.* (2001)
Yellow Sea		3.9	1.3	10.5			88.2	benzene	Takeda *et al.* (2004)
Coastal									
Biscayne Bay, FL	9.7 ± 1.2	24.4 ± 3.0	2	ND	2		96	methanol	Mopper & Zhou (1990)
10% Everglades water in Biscayne Bay water	30.1	68.9						methanol	Mopper & Zhou (1990)
Vineyard Sound, MD	10.6	26.5						methanol	Mopper & Zhou (1990)
Paradise Harbor, Antarctica	4.3	0.53	~33	67			67	benzoic acid	Qian *et al.* (2001)
Seto Inland Sea		15.3	0.1	6.8	0.5		92.6	benzene	Takeda *et al.* (2004)
Taira Bay, Japan (red-soil polluted, iron-rich water)		9	2.9	30.1	1	63		benzene	Arakaki *et al.* (2009)
Deeper Waters									
Open-ocean									
Sargasso Sea (>700 m)	6.3 ± 0.3	15.9 ± 0.7	19	1	3		77	methanol	Mopper & Zhou (1990)
Gulf Stream (700 m)	5.8	14.7						methanol	Mopper & Zhou (1990)
Crystal Sound, Antarctica (20 m)	0.18	0.02	~25	73			73	benzoic acid	Qian *et al.* (2001)
Yellow Sea (60 m)		7.2	6.7	44.2			49.1	benzene	Takeda *et al.* (2004)
Coastal									
Paradise Harbor, Antarctica (15 m)	0.031	0.004	~25	73			73	benzoic acid	Qian *et al.* (2001)
Seto Inland Sea (30 m)		49.5	1.2	74.5	0.1		24.1	benzene	Takeda *et al.* (2004)

Table A-2: Reported $HO^{\bullet}$ Steady State Concentrations, Formation Rates, and Source Contributions in Surface Waters of Varying Type

Sample Description	$[HO^{\bullet}]_{ss}$ $\times 10^{-16}$ M	$HO^{\bullet}$ formation rate $\times 10^{-12}$ M s^{-1}	$HO^{\bullet}$ formation from different sources (%)					Probe Method	Reference
			NO_3^-	NO_2^-	H_2O_2	Fenton	Other (DOM)		
Rivers									
Kurose, Ohta, Seno, Ashida and Oze Rivers, Japan (mean values)		56.1	33	31	<1	15	20	benzene	Nagatani *et al.* (2007)
Ohta River, Japan (upstream)		10.1	1.6	10.2	0.7		87.5	benzene	Takeda *et al.* (2004)
Ohta River, Japan (downstream)		25.9	23.0	25.6	0.3		51.1	benzene	Takeda *et al.* (2004)
Kurose river, Japan (upstream)		17.5	19.1	5.9	0.4		74.7	benzene	Takeda *et al.* (2004)
Kurose river, Japan (downstream)		146.3	18.7	47.6	0.1		33.7	benzene	Takeda *et al.* (2004)
Blue Earth River, MN	9.9							butyl chloride	Brezonik *et al*. (1998)
Lakes (near surface)									
Lake Minnetonka, MN	0.31							butyl chloride	Brezonik *et al*. (1998)
Lake Nichols, WI	0.25							butyl chloride	Brezonik *et al*. (1998)
Avigliana Grande, Italy	3.8	24						benzene	Vione *et al.* (2010)
Avigliana Piccolo, Italy	2.3	13						benzene	Vione *et al.* (2010)
Lago Blu, Italy	0.72	5.4						benzene	Vione *et al.* (2010)
Viverone, Italy	0.19	4.7						benzene	Vione *et al.* (2010)
Meugliano, Italy	0.98	40						benzene	Vione *et al.* (2010)
Soprano, Italy	0.75	12						benzene	Vione *et al.* (2010)
Sottano, Italy	1.2	3.2						benzene	Vione *et al.* (2010)
Laghetto, Italy	0.80	7.9						benzene	Vione *et al.* (2010)
Greifensee Lake	3	10						butyl chloride	Haag and Hoigne (1985)

Appendix B

Results from Preliminary Research Regarding the Formation of Reactive Oxygen Species from Macondo Crude Oil

In this research, preliminary experiments were conducted to quantify the formation rates of $HO^{\bullet}$ and singlet oxygen ($^1O_2$) from crude oil films. All experiments were conducted using solar simulation. For the $HO^{\bullet}$ experiments, the crude oil film was added to ultrapure water. No additional probe compound was added in order to observe if the benzene in the oil would serve as an internal $HO^{\bullet}$ probe. For the $^1O_2$ experiments, the crude oil film was added to ultrapure water amended with 21.9 μM furfuyl alcohol as the probe compound to monitor $^1O_2$ formation. In all experiments, samples were placed in a 70 mm diameter crystallization dish, covered with a pyrex lid, and placed in a chilled water bath to maintain a constant solution temperature of 20°C. Sample aliquots were collected in duplicate by drawing liquid from the water solution; any oil present in the sample was removed after a 30 min equilibration period in a separation funnel. Samples were transferred to 2 mL vials and analyzed using HPLC-UV for the corresponding probe compound.

The results from the $HO^{\bullet}$ preliminary experiments are shown in Figure B-1. After 3.5 hours of irradiation, the amount of phenol increases from 60 peak area units to 730 peak area units. This increase in phenol indicates that benzene present in the oil will serve as an internal probe for $HO^{\bullet}$ formation and that some $HO^{\bullet}$ is being formed from the oil.

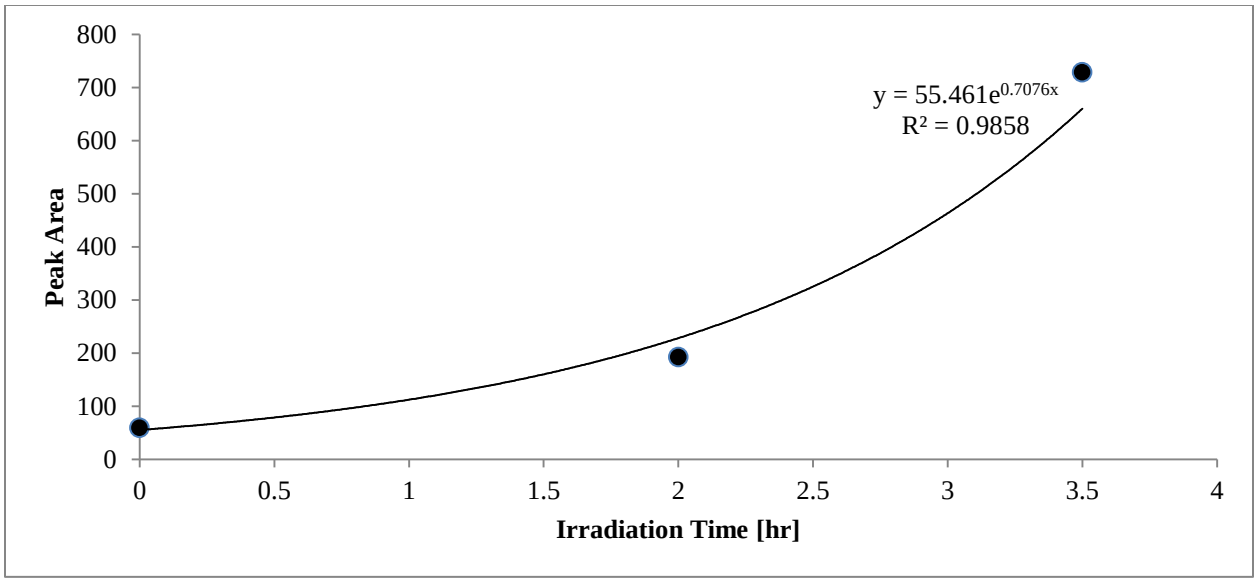

Figure B-1: Formation of phenol from irradiated crude oil indicates formation of hydroxyl radical. Data were fit with an exponential trendline to quantify the formation rate expressed as HPLC-UV detectable peak area units.

The cumulative results from three $^1O_2$ experiments are presented in Figure B-2. Here, photoproduction rates of $^1O_2$ and the corresponding $[^1O_2]_{ss}$ have been plotted as a function of oil film thickness. These data points were determined from three separate experiments in which ultrapure water amended with furfural alcohol and covered by an oil film (6 mL, 12.5 mL, 25 mL) was irradiated using solar simulation for up to 4 hours. These results confirm previous work by Correa *et al.* (2012) that $^1O_2$ is formed from crude oil upon exposure to sunlight. These results also present a hypothesis regarding the formation location of the $^1O_2$ from the oil film. Because the $^1O_2$ photoproduction rate decreases with increasing oil film thickness, these results suggest that $^1O_2$ may be formed at the oil surface and is controlled by diffusion as the $^1O_2$ must travel through the entire oil film to reach the oil-water interface where it can react with the probe compound. Further research is needed to confirm this hypothesis such as the measurement of crude oil absorption spectrums and the extensions of experiments to include thicker oil films.

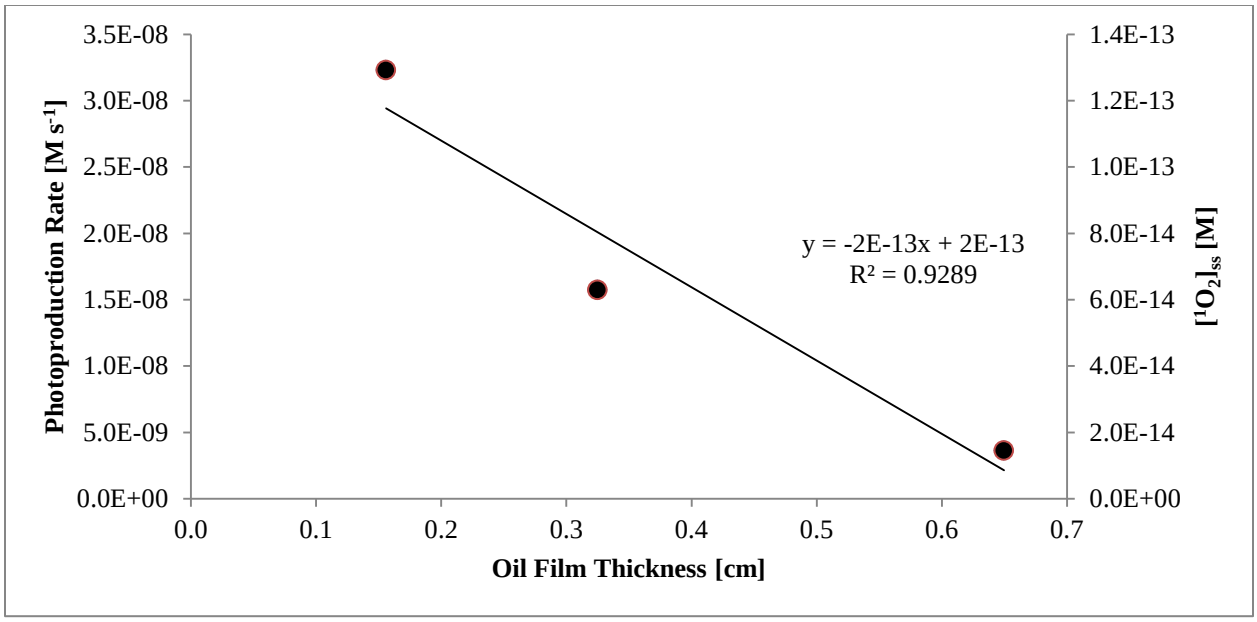

Figure B-2: Singlet oxygen production as a function of film thickness. The secondary axis shows the corresponding singlet oxygen steady-state concentration as a function of film thickness. These data points were determined from three separate experiments in which ultrapure water covered by an oil film (6 mL, 12.5 mL, 25 mL) was irradiated using solar simulation for up to 4 hours. Furfural alcohol was used as the probe compound to detect singlet oxygen by HPLC-UV.

Appendix C

Method of Relative Standard Deviation Calculations for Propylene Glycol and 2-Butoxyethanol Concentrations Detected by GC-FID

Relative standard deviation (RSD) as a function of reported GC-FID peak area and as a function of concentration were determined for both PG and 2-BE based on standard deviations at concentrations near the MDL and at 50 mg L^{-1}. For PG, the RSD at the lower end of detection (n = 7, [PG] = 25 mg L^{-1}) is 4% and is 16% at the experimental spike concentration of 50 mg L^{-1} (n = 18). For 2-BE, the RSD at the lower end of detection (n = 7, [2-BE] = 5 mg L^{-1}) is 3% and is 10% at the experimental spike concentration of 50 mg L^{-1} (n = 23). Exponential trendlines were fit to these values to create a variable RSD that could be applied to different detected peak areas or concentrations (Table C-1).

Table C-1: Relative standard deviation (RSD) determination. Equations expressed as a function of peak area and as a function of concentration.

Chemical name	Equation	Average PA	Concentration (mg L^{-1})	n	RSD
Propylene glycol (PG)	$RSD(PA) = 0.0068e^{0.1751PA}$	10.5	25	7	4%
	$RSD([C]) = 0.0109e^{0.0543[C]}$	18.2	50	18	16%
2-Butoxyethanol (2-BE)	$RSD(PA) = 0.0206e^{0.0399PA}$	5.5	5	7	3%
	$RSD([C]) = 0.0220e^{0.0309[C]}$	40.4	50	23	10%

PA: peak area; [C]: concentration

The results of some experiments conducted in this study were determined to be unreportable due to the large standard deviations (σ) associated with the GC-FID method of compound detection. Figure C-1 illustrates an instance of this unreportability for experiments regarding PG. This experiment was an additional competition kinetics experiments that was performed to determine k_{HO}**.** values for the target compound. The experimental method was similar to that previously described in the Methods and Materials section with the following experimental parameter changes: $[PG]_0$ = 0.75mM = 57.07 mg L^{-1}; $[pCBA]_0$ = 0.75 mM = 117.43 mg L^{-1}, $[H_2O_2]_0$ = 0.75 mM = 25.51 mg L^{-1}. Sample aliquots were sacrificed at UV doses of 0, 100, 200, 300, and 400 mJ cm^{-2}.

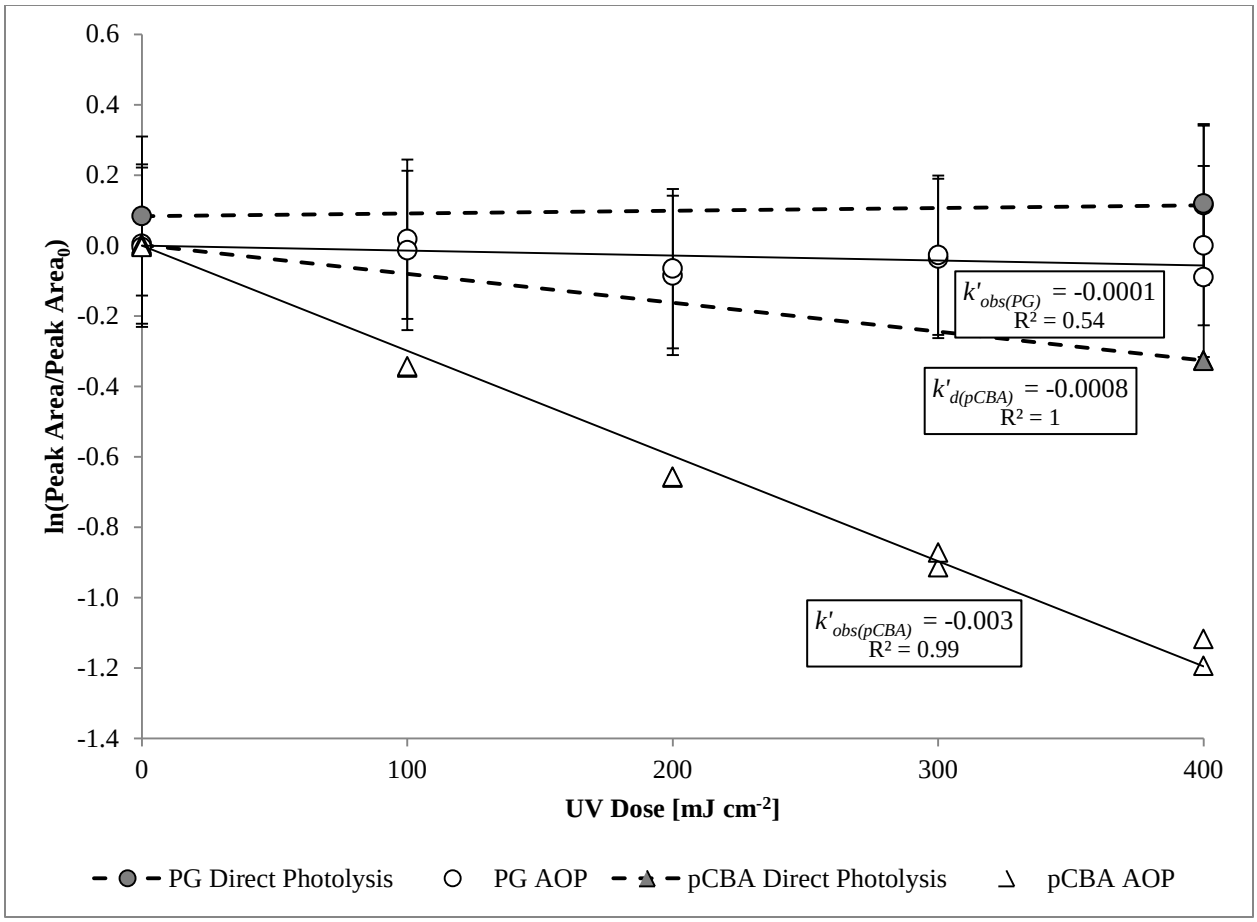

Figure C-1: Importance of inherent standard deviation in reporting results of a propylene glycol (PG) competition kinetics experiment. The error bars on the PG data points (circle) demonstrate the impact of the large variability of the GC-FID method on experimental results. Error bars represent the σ determined from the appropriate RSD for each detected peak area. Experimental parameters: $[PG]_0$ = 0.75 mM, $[pCBA]_0$ = 0.75 mM. Grey data points connected by dashed lines indicate results from direct photolysis. Open data points connected by solid lines indicate results from AOP experiments ($[H_2O_2]_0$ = 0.75 mM).

The degradation trend from the PG experiment (Figure C-1) is easily dismissed without an examination of σ due to the poor coefficient of correlation (R^2 = 0.54), indicating a non-trend in degradation. When data points are corrected for GC-FID variability with the application of an appropriate σ to each data point (based on the developed RSD equations as a function of peak area), the lack of a statistically significant trend is further confirmed.

The high variability in peak area reporting of the GC-FID method makes the method an obvious undesirable choice for precision analysis. It is important that all reported experimental

results obtained using the GC-FID method are analyzed for statistical significance in spite of the inherent high standard deviations, and that the σ of each sample is carried throughout all mathematical data manipulations. This was done for all PG and 2-BE experimental results presented in this study. Any lack of observable error bars on figures is due to low final σ value.